Picket-fence ruthenium(II) phthalocyaninates bearing (1R,2S,5R)menthoxy-groups for chiral surrounding of the metal center

Andrey Kroitor, Anna Sinelshchikova, Mikhail Grigoriev, Gayane Kirakosyan, Alexander Martynov, Yulia Gorbunova, Alexander Sorokin

Picket-fence ruthenium(II) phthalocyaninates bearing (*1R,2S,5R*)-menthoxy-groups for chiral surrounding of the metal center

Andrey P. Kroitor[a], Anna A. Sinelshchikova[a], Mikhail S. Grigoriev[a], Gayane A. Kirakosyan[a,b], Alexander G. Martynov[a,*], Yulia G. Gorbunova[a,b,*], Alexander B. Sorokin[c,*¶]

[a] *Frumkin Institute of Physical Chemistry and Electrochemistry, Russian Academy of Sciences, Leninskii pr., 31, bldg. 4, 119071, Moscow, Russia. E-mail: martynov@phyche.ac.ru*

[b] *Kurnakov Institute of General and Inorganic Chemistry, Russian Academy of Sciences, Leniskii pr., 31, 119991 Moscow, Russia. E-mail: yulia@igic.ras.ru*

[c] *Institut de Recherches sur la Catalyse et l'Environnement de Lyon IRCELYON, UMR 5256, CNRS - Université Lyon 1, 2 av. A. Einstein, 69626 Villeurbanne, France. E-mail: alexander.sorokin@ircelyon.univ-lyon1.fr.*

Dedicated to Prof. Irina P. Beletskaya on the occation of her 90th Birthday

Abstract:

We report design and synthesis of novel picket fence phthalocyanines to access the ruthenium(II) complexes carrying di-(*1R,2S,5R*)-menthoxy -substituted aryloxy-groups. Owing to bulkiness of such groups located either at peripheral (β) or non-peripheral (α) positions, they are nearly orthogonal to the plane of the phthalocyanine thus creating a chiral environment around the metal center. This orthogonality was supported by X-ray analysis of corresponding phthalonitrile precursors (86.0° and 81.4° angles between the planes of aromatic moieties for α- and β-substituted phthalonitriles, respectively). As a proof of concept, the synthesized complexes were investigated as catalysts in a benchmark reaction of the cyclopropanation of styrene by ethyl diazoacetate. While the β-substituted complex showed very low enantioselectivity, the α-substituted analogue afforded a moderate asymmetric induction towards ethyl (*1S,2R*)-2-phenylcyclopropane-1-carboxylate. This result emphasizes the importance of appropriate arrangement of the chiral groups relative to the phthalocyanine catalytic center and provides guidelines for further elaboration of phthalocyanine catalysts for asymmetric transfer of carbenes.

Keywords: phthalocyanine, ruthenium, menthol, carbene transfer, cyclopropanation, enantioselectivity.

1. Introduction

Enantioselective functionalization of organic compounds typically requires chiral catalysts [1,2]. Chiral metal complexes occupy a place of choice for many asymmetric reactions such as

epoxidation [3–5], oxidation of C-H bonds [6,7], nitrene [8] and carbene [9–11] transfers, etc. In particular, a large variety of chiral porphyrin complexes have been prepared and successfully used as catalysts for enantioselective reactions [12–19]. Among them, metal-mediated asymmetric carbene transfer reactions is a powerful tool in organic synthesis, notably, for the production of chiral cyclopropane fragments that are encountered in a vast number of biologically active compounds [20]. According to detailed mechanistic studies, the carbene transfer reactivity is associated with the involvement of metal carbene species which can be typically generated from diazo compounds used as carbene precursors [7-9]. Among a large number of catalysts for such reactions, tetrapyrrolic molecules, mainly porphyrins, attract particular interest due to the structural versatility, robustness, high turnover numbers and low catalyst loadings in comparison with other coordination compounds.

To achieve an asymmetric induction for cyclopropanation of olefins catalyzed by porphyrins and their derivatives, three general strategies can be employed. One of them implies the application of engineered cytochrome P-450, which has been developed by a direct evolution of several hemoproteins containing iron in a catalytic site [21–26]. Another method involves the artificial enzymes, contains unnatural co-factors [27–30]. In that case, other metals and ligands apart from heme can be used, but toolbox of possible macrocycles still has significant restrictions. It should be emphasized that in both cases the enantioselective outcome of reactions is provided by the apoenzyme structure and the preparation of such catalysts relies mainly on biotechnological approaches.

Otherwise, a chemical strategy implies the synthesis of catalysts bearing chiral groups attached directly to the tetrapyrrolic core providing therefore asymmetric induction. This method makes it possible to expand the set of catalysts by moving from the heme archetype to a wide range of abiogenic ligands and metals. For instance, porphyrinoids bearing chiral groups, in which iron [19,31–39], ruthenium [32,37,40–55], rhodium [56–60], iridium [61] or cobalt [18,62–69] are embedded, demonstrate high catalytic activity in stereoselective carbene transfer to C=C bonds [8]. In particular, Che et al. reported cyclopropanation of styrene (5 equiv) by EDA (1 equiv) mediated by the chiral Ru Halterman porphyrin complex (0.05 mol%) with 83 % yield, *trans/cis* ratio of 18:1 and 87% e.e [52]. Zhang and coworkers developed a series of chiral Co porphyrins which cyclopropanate styrene (1 equiv) by EDA (1.2 equiv) with 2 mol% catalyst loading with 57-95 % yield, with *trans/cis* ratio ranging from 32:68 to 96:4 and 31-89% e.e

[66]. Simonneaux and coworkers obtained a 52% product yield with 96:4 diastereoselective ratio and 83% e.e. in the reaction of styrene (5 equiv) with EDA (1 equiv) in the presence of 0.5 mol% of Ru sulfonated Halterman porphyrin [38].

Various concepts are used in the literature to describe the architecture of chiral porphyrinoid catalysts, including the frequently used *picket-fence*, and sporadic examples of the concepts *chiral wall* [57] or *chiral fortress* [59]. Notably, the first concept was used by Collman et al. for complexes containing bulky substituents on only one side relative to the plane of the macrocyclic backbone [70,71]. However, the application of picket-fence term was further extended to complexes containing chiral substituents on both sides relative to the plane of the macrocycle [72–74].

The porphyrin counterparts – phthalocyanines (Pc) exhibit high catalytic activity in a wide range of reactions [75], however they are virtually unexplored in enantioselective catalysis despite a number of complexes containing chiral substituents [76], including aliphatic [77,78], binaphthyl [79,80], carbohydrate [81] or aminoacid groups [82]. Only three papers have reported chiral reactions in the presence of phthalocyanine complexes. The Zn(II) and Co(II) complexes bearing four chiral hydrobenzoin groups (2.5-5 mol% catalyst loading) mediated interaction of diethylzinc and aldehydes with low yields of secondary alcohols (5-38 %) and 7-33 % *ee* [83,84]. High enantioselectivity induced by protein was achieved for non-covalent conjugate of bovine serum albumin and sulfonated Cu(II) phthalocyanine catalyzing Diels-Alder reaction with 85-98 % *ee* [85]. However, to the best of our knowledge phthalocyanine complexes have never been used in asymmetric carbene transfer including cyclopropanation.

A literary survey shows that in all reported chiral phthalocyanine complexes chiral substituents are coplanar with the macrocycle plane. For example, this structural feature was observed in several (*1R,2S,5R*)-menthoxy-substituted phthalocyanines (Fig. 1a) [86–93]. Consequently, it is doubtful that catalytically active phthalocyanines with such geometry will provide enantioselective induction since the chiral groups are remote from the catalytic metal center. To overcome this obstacle, in the present work we took advantage of “picket fence” architecture for chiral phthalocyanine catalysts as it can bring sterically hindered chiral groups above and below macrocycle plane in proximity to the metal center (Fig. 1b). Ruthenium(II) phthalocyaninate was selected as a catalytically active core since achiral RuPc have already demonstrated high catalytic activity in carbene transfer [94–97].

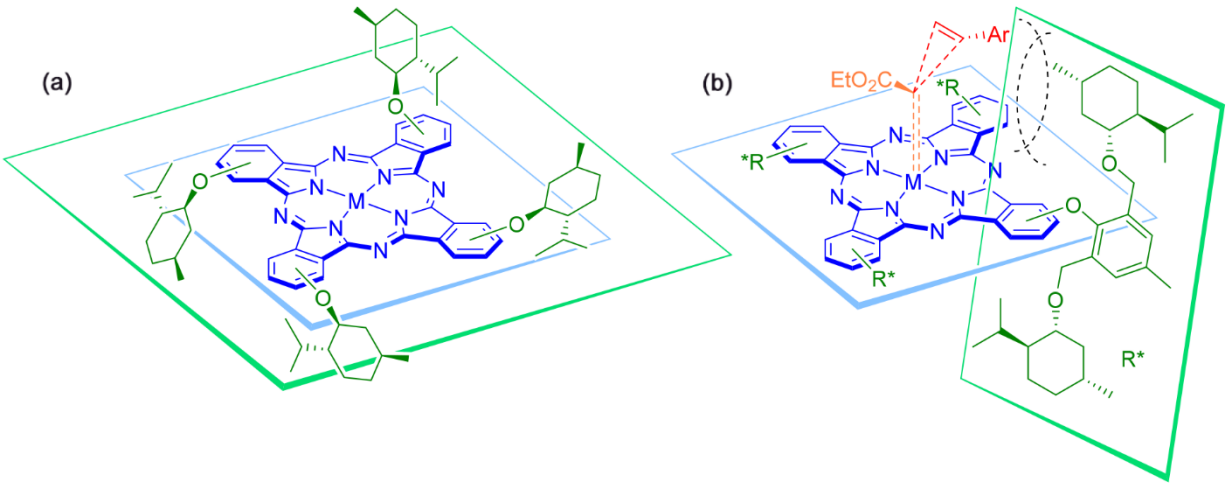

Fig. 1. (a) Reported (*1R,2S,5R*)-menthoxy-substituted phthalocyanines[86–93] whose chiral groups are positioned in a plane of macrocycle core; (b) our proposed design for the new aryloxy-substituted phthalocyanine complex with picket-fence architecture where chiral (*1R, 2S,5R*)-menthoxy-fragments are placed orthogonally with respect to the macrocyclic backbone.

2. Results and discussion

To leverage the picket-fence architecture, we designed the bis-*ortho*-aryloxy-substituted phthalocyanines where the chiral groups will be placed above and below the macrocycle plane. The readily available 2,6-*bis*-(hydroxymethyl)-*p*-cresol has been used as a precursor of such phthalocyanines since its aliphatic hydroxyl groups can be easily functionalized via reactions with nucleophiles [98–100]. In the present work we first used naturally occurring (*1R,2S,5R*)-menthol as such a nucleophile, thus obtaining the first examples of chiral picket fence phthalocyanines, whose catalytic activity was tested using cyclopropanation reactions as an example (Fig. 1b). Henseforward we will use the term "menthol" without indication of configurations of each stereocenter for simplicity, as these configurations will not change upon further chemical reactions.

Thus the reaction of 2,6-*bis*-(hydroxymethyl)-*p*-cresol with 15-fold excess of menthol in melt was performed at 150°C (Fig. 2). It was shown that substitution of labile hydroxy groups at benzylic positions with menthyl residues proceeds without any catalyst. The excess of unreacted menthol was recovered by vacuum distillation and the target phenol bearing two menthoxymethyl groups **Ar*OH** was isolated in a 45% yield after chromatographic purification (Fig. S1-S8).

The 1H NMR spectrum of Ar*OH exhibits two doublet signals of diastereotopic protons of benzylic methylene groups CH_aH_b at ca. 4.8 and 4.5 ppm with a geminal constant J = 11.9 Hz (Fig. 2a). This coupling was revealed by the presence of cross peaks in the ^{1}H-^{1}H COSY NMR

spectrum (Fig. S4). The ^{1}H-^{13}C HSQC spectroscopy demonstrated that both protons are coupled with the same carbon atom (Fig. S5).

Next, the phenol **Ar*OH** was treated with 3- or 4-nitrophthalonitriles in the presence of K_2CO_3 in DMF which resulted in smooth substitution of NO_2 groups by aryloxy moieties. These reactions provided the corresponding α- and β-Ar*O-substituted nitriles in high yields of ~60% (Fig. 2). The structure of isolated compounds was confirmed by NMR, HR-ESI and FT-IR (Fig. S9-S24).

The interesting feature of the synthesized phthalonitriles was noted in their NMR spectra. The resonance signals of benzylic protons in **(β-Ar*O)Pn** appeared as a couple of doublets similarly to the spectrum of **Ar*OH** (Fig. 2c). In the contrast, in the case of α-substituted counterpart four benzylic doublets were observed and they nearly coalesced upon heating of the sample above 80 °C in toluene-d_8 (Fig. 2b) This observation can evidence a hindered rotation of chiral aryloxy-group when it is located in the α-position of the phthalonitrile moiety. In the case of **(β-Ar*O)Pn** this rotation is fast on NMR timescale and cooling to -80 °C was required to observe the splitting of benzylic resonance signals (Fig. 2c).

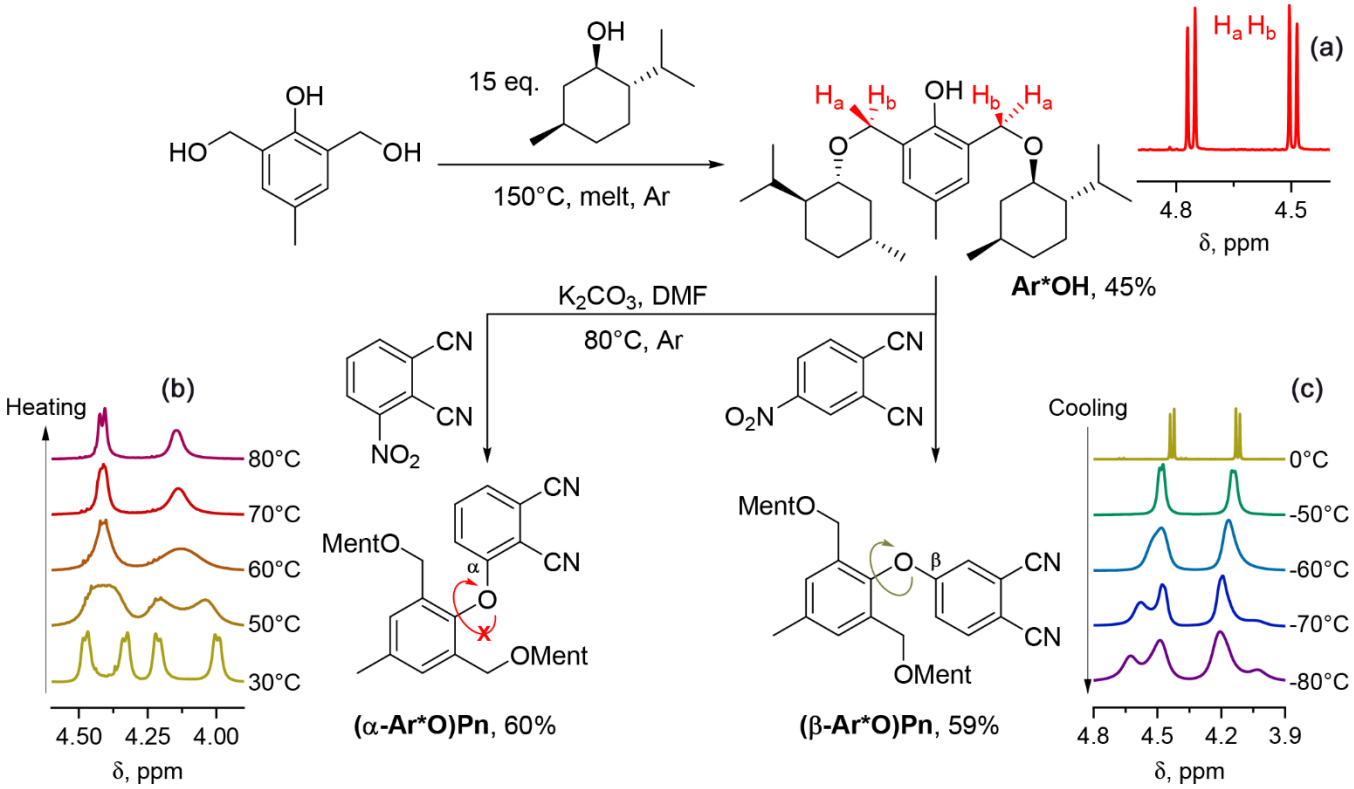

Fig. 2. Synthesis of menthoxymethyl-subtituted phenol and phthalonitriles. Abbreviation "Ment" stands for (*1R,2S,5R*)-menthyl group. Inset (a) shows the resonance signals of benzylic protons in ^{1}H-NMR spectrum of phenol **Ar*OH** in $CDCl_3$. Insets (b) and (c) show resonance

signals of benzylic protons in variable temperature ^{1}H-NMR spectra of phthalonitriles **(α-Ar*O)Pn** and **(β-Ar*O)Pn** in toluene-d_8 respectively.

The synthesized phthalonitriles were characterized by the single-crystal XRD (Fig. 3, Tables S1-S7). In crystalline phase the phthalonitrile groups are almost orthogonal to the aryloxy-fragments with chiral substituents with torsional angles of 86º and 81º for α- and β-substituted phthalonitriles respectively.

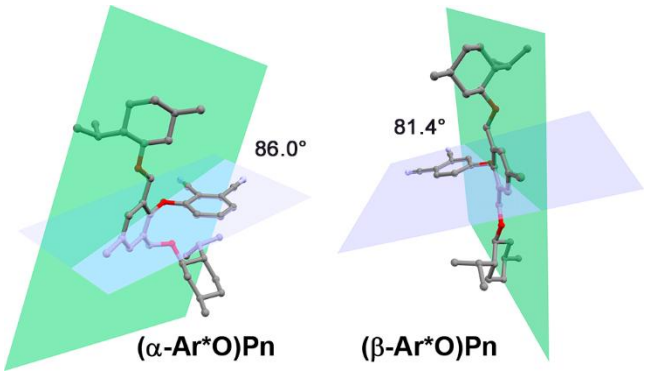

Fig. 3. Single crystal XRD structures of phthalonitriles **(α-Ar*O)Pn** (left) and **(β-Ar*O)Pn** (right). The torsional angles between the phthalonitrile fragment and the aryloxy group are indicated. Hydrogen atoms are omitted for clarity.

Assuming the results of VT-NMR for these nitriles, we can anticipate that such orthogonality is likely to be presumed in solution for **(α-Ar*O)Pn** and phthalocyanine derived from it, while β-substituted compounds might exist in solution as a set of conformers.

Template condensation of phthalonitriles in the presence of magnesium turnings in refluxing pentanol afforded corresponding Mg(II) phthalocyaninates as inseparable mixtures of positional isomers which bear four chiral aryloxy groups in non-peripheral (α) and peripheral (β) positions **Mg[(α-Ar*O)$_4$Pc]** and **Mg[(β-Ar*O)$_4$Pc]**. The formation of complexes was evidenced by MALDI TOF MS and UV-Vis techniques (Fig. 4a, Fig. S25-28). Further treatment of Mg(II) complexes with an aqueous solution of trifluoroacetic acid resulted in the formation of metal free ligands **H$_2$[(α-Ar*O)$_4$Pc]** and **H$_2$[(β-Ar*O)$_4$Pc]** obtained in good yields based on corresponding phthalonitriles (59% and 43%, respectively) (Scheme 1). The formation of the phthalocyanine ligands was confirmed by UV-Vis, FT-IR and ^{1}H NMR spectroscopies (Fig. S30-S32, S33-S35). The Q-bands of α-substituted phthalocyanine and its magnesium complex in the UV-Vis spectra are bathochromically shifted by ~20 nm in comparison with β-substituted compounds (Fig. 4). Such a bathochromic shift was previously observed in the case of peripheral and non-peripheral ruthenium octa-*n*-butoxyphthalocyanines [97].

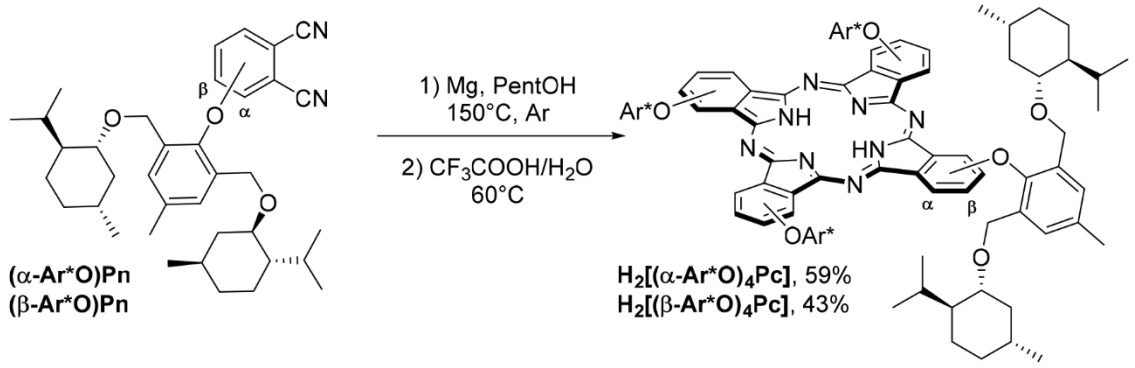

Scheme 1. Synthesis of phthalocyanines **H_2[(α-Ar*O)$_4$Pc]** and **H_2[(β-Ar*O)$_4$Pc]**.

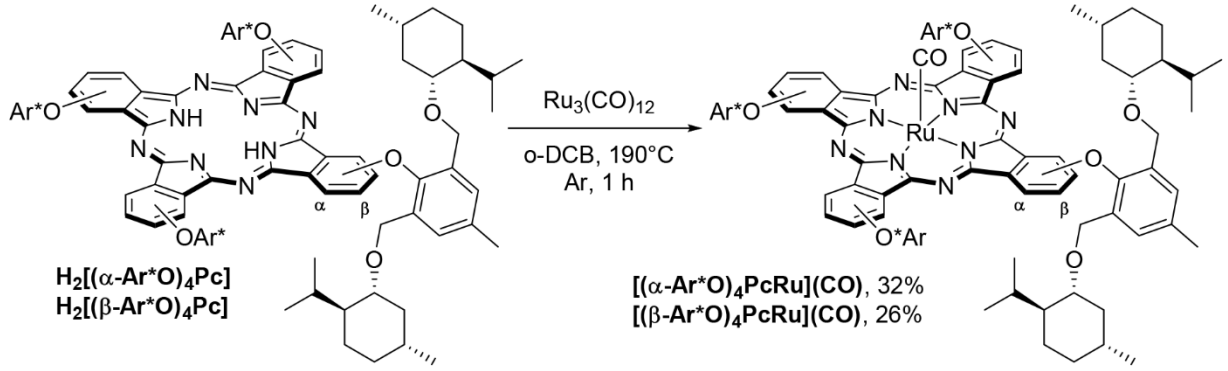

Scheme 2. Synthesis of ruthenium(II) phthalocyaninates **[(α-Ar*O)$_4$PcRu](CO)** and **[(β-Ar*O)$_4$PcRu](CO)**.

Next, the insertion of ruthenium into phthalocyanines was performed using $Ru_3(CO)_{12}$ in refluxing *o*-dichlorobenzene similar to the previously described protocol [95,97,101]. The separation of the reaction products by size-exclusion chromatography revealed the formation of monomeric complexes **[(α-Ar*O)$_4$PcRu](CO)** and **[(β-Ar*O)$_4$PcRu](CO)**. Owing to the difficulties in the separation of ruthenium phthalocyanines from unreacted starting ligands, the column purification had to be carried out several times, resulting in moderate preparative yields of the target products (32% and 26%, respectively) (

, Fig. S36-S43). The HR ESI mass spectra of complexes **[(α-Ar*O)$_4$PcRu](CO)** and **[(β-Ar*O)$_4$PcRu](CO)** showed the intense signals of protonated molecular ions with isotopic distribution pattern of molecular peaks identical to that of calculated one (Fig. S37 and S41). The UV-Vis spectra of ruthenium phthalocyanines shows the intense narrow Q-bands which is shifted from 659 nm for macrocycle bearing substituents at peripheral positions to 673 nm for the non-peripherally substituted compound (Fig. 4). The presence of axial CO ligand was confirmed by FT-IR spectroscopy due to the presence of ν^{CO} bands at 1967 and 1962 cm^{-1} for α- and β-substituted complexes (Fig. S39 and S43).

The inherent problem in the synthesis of tetrasubstituted phthalocyanines is the formation of the positional isomers C_{4h}, C_s, C_{2v} and D_{2h} in a 1:4:2:1 statistical ratio in the case of non-bulky substituents. Their separation is tedious and cannot be often realized on a practical scale. The isolation of one or more regioisomers was published in rare cases [102–105]. In principle, we could expect the preferable formation of the less-sterically hindered C_{4h} α-substituted isomer in template condensation of **(α-Ar*O)Pn**, however the complicated group of overlapping signals in NMR spectra of α-substituted macrocycles (Fig. S31 and S38) suggests that the mixture of isomers was obtained. Unfortunately, all our attempts to separate this mixture or isolate at least one isomer by column chromatography using different solvents and sorbents (SiO_2, Brockmann I and IV neutral Al_2O_3, Bio-Beads S-X1) have failed, neither separation of products on TLC was observed.

It should be noted that ruthenium phthalocyanines containing aryloxy groups are still rare. Yanagisawa et al. reported the preparation of A_3B-type complexes bearing the residue of 4-hydroxybenzoic acid at peripheral positions [106]. We have recently published the preparation of **[(β-MesO)$_8$PcRu](CO)** [101] and its application in a carbene transfer reactions [96]. To the best of our knowledge, complexes **[(α-Ar*O)$_4$PcRu](CO)** and **[(β-Ar*O)$_4$PcRu](CO)** are the first example of ruthenium phthalocyanines containing *four* aryloxy-groups.

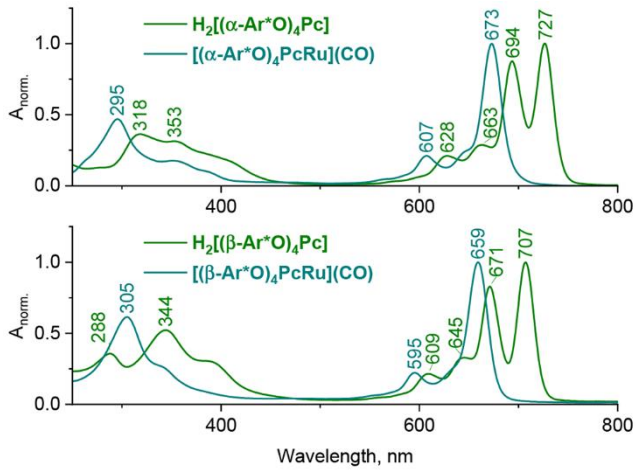

Fig. 4. UV-Vis spectra of metal-free phthalocyanines **H_2[(α- or β-Ar*O)$_4$Pc]** and ruthenium(II) complexes **[(α- or β-Ar*O)$_4$PcRu](CO)**.

Both chiral ruthenium phthalocyanine complexes were initially evaluated in catalytic cyclopropanation of styrene with ethyl diazoacetate (EDA) using 0.1 mol% catalyst loading in dichloromethane. To limit the formation of the EDA dimerization products (diethyl maleate and diethyl fumarate), the EDA solution was slowly added to the reaction mixture by syringe pump. It should be noted that the non-peripheral **[(α-Ar*O)$_4$PcRu](CO)** complexes showed a higher diastereoselectivity with a *trans/cis* ratio of 5.6:1 in comparison with a 4.7:1 ratio for the peripheral **[(β-Ar*O)$_4$PcRu](CO)** complex. The cyclopropanation mediated by the peripherally substituted **[(β-Ar*O)$_4$PcRu](CO)** complex resulted in the negligible enantiomeric excess of *trans*-isomer whereas in the presence of the non-peripheral **[(α-Ar*O)$_4$PcRu](CO)** complex with chiral substituents closer to metal center an enantiomeric excess of 10% was obtained for *S,R*-cyclopropanation product of *cis*-isomer (Scheme 3).

Thus, the complex bearing *four* chiral groups at non-peripheral positions showed a better enantioselectivity in comparison with the β-substituted counterpart. To achieve a higher asymmetric induction we tried to prepare phthalocyanine bearing *eight* chiral groups *at non-peripheral positions*. To this aim, 3,6-difluorophthalonitrile was prepared according to the previously described protocol of selective reduction of tetrafluorophthalonitrile with $NaBH_4$ using an equivalent amount of water [107]. – ***was replaced to Conclutuon***

The reaction of 3,6-difluorophthalonitrile with 5 eq. of phenol **Ar*OH** proceeded smoothly for 3 h at 80ºC and afforded the target *bis*-aryloxy-substituted phthalonitrile **(α-Ar*O)$_2$Pn** in the excellent yield (93%) (Scheme 4), its structure was confirmed by NMR and FT-IR (Fig. S46-49). It should be noted that the excess of **Ar*OH** can be reduced to 2.1 eq.

without lowering the reaction efficiency. Unfortunately, a template condensation of this phthalonitrile in the presence of magnesium or lithium turnings or $Mg(OAc)_2$ with DBU in refluxing dry pentanol did not result in even traces of phthalocyanine. Similarly, previous studies showed that the presence of two bulky substituents in non-peripheral positions prevents the formation of octa-substituted phthalocyanines and their synthesis still a formidable challenge [108]. ***To be replaced to SI***

Thus, the cyclopropanation reaction was further optimized using **[(α-Ar*O)$_4$PcRu](CO)** as the catalyst. First of all, we found that the enantioselectivity of cyclopropanation reaction strongly depends on the solvent nature (Table 1).

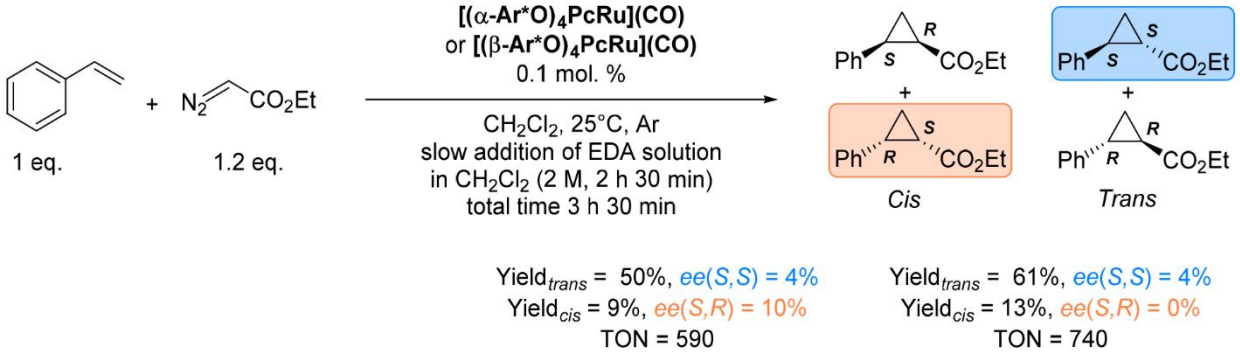

Scheme 3. Cyclopropanation of styrene with EDA catalyzed by chiral ruthenium phthalocyanines **[(α-Ar*O)$_4$PcRu](CO)** and **[(β-Ar*O)$_4$PcRu](CO)**.

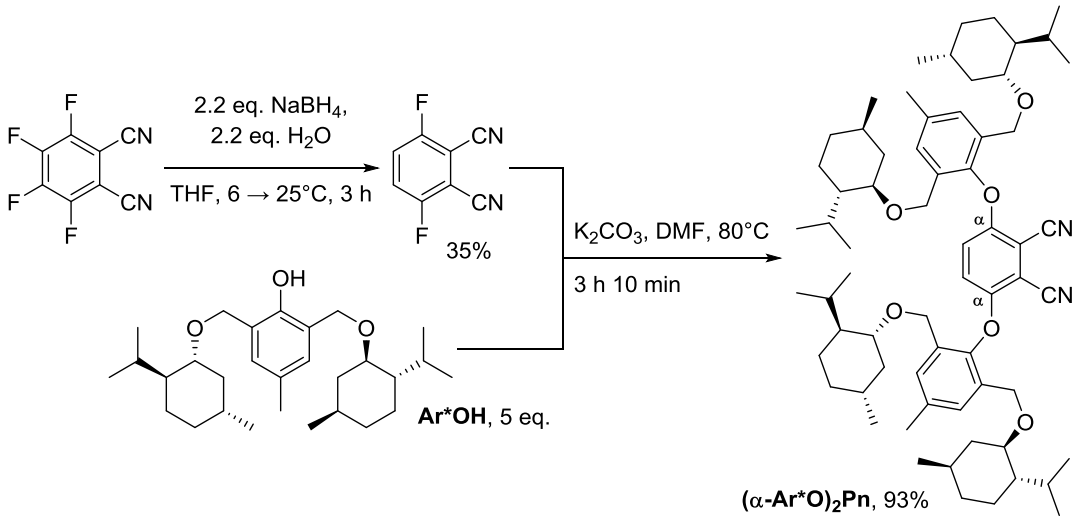

Scheme 4. Synthesis of 3,6-*bis*-aryloxy-substituted phthalonitrile **(α-Ar*O)$_2$Pn**. ***To be replaced to SI***

Table 1. Cyclopropanation of styrene by EDA catalyzed by chiral ruthenium phthalocyanine **[(α-Ar*O)$_4$PcRu](CO)** in different solvents. [a]

Solvent	Cyclopropanation yield, % [b]				Enantiomeric excess, % [c]	
	trans	*cis*	*trans*/*cis*	TON	*trans* (S, S)	*cis* (S, R)
CH_2Cl_2	50	9	5.6:1	590	4	10
Toluene	67	14	4.9:1	670	4	14
CH_3CN	0	0	0	0	0	0
Ethyl acetate (EtOAc)	80	12	6.7:1	800	8	16
Propylene carbonate	86	14	6.1:1	860	6	12
DMF	27	3	9:1	270	8	11
Dimethyl acetamide (DMA)	62	7	8.9:1	620	9	16
2-pyrrolidinone	75	10	7.5:1	750	8	16
iso-amyl acetate	25	3	8:1	250	6	16
tert-butyl acetate (*t*BuOAc)	58	8	7.3:1	580	8	18
tert-butyl acetoacetate	79	14	5.6:1	790	8	8
*t*BuOAc/DMA = 1/1 (vol. %)	80	13	6.2:1	800	8	15
*t*BuOAc [d]	18	3	6:1	180	12	16

[a] Conditions: 0.25 mmol styrene, 0.3 mmol EDA (addition time: 2.5 h), 0.25 mL solvent, Ar, 25°C, reaction time: 3.5 h. [b] Yields were determined by ^{1}H NMR and based on styrene amount. [c] Enantiomeric excesses were determined by GC-MS using the chiral column CycloSil-B. [d] Reaction was performed at 0°C.

In particular, diastereomeric ratios range from 4.9:1 in toluene to 9:1 in dimethylformamide. No reaction was observed in acetonitrile. The replacement of CH_2Cl_2 with toluene increased *ee* for *cis*-isomer to 14%. Using of propylene carbonate solvent provided the high product yield (86 %), *trans/cis* ratio of 6:1:1 and *ee* of 12 %. Interestingly, ethyl acetate provided the best results for asymmetric induction: *ee*(*trans*) = 8% and *ee*(*cis*) = 16% while keeping good product yield and diastereoselectivity. Further screening of alkyl acetates showed that in *tert*-butyl acetate the enantiomeric excess of (*S,R*)-isomer reached 18%. Decrease of the reaction temperature to 0°C resulted in lower conversion without increase of the *ee* for *cis*-isomer though *ee* of trans-isomer was slightly increased to 12 %. When the 1:1 mixture of *t*BuOAc/DMAA was used no increase of diastereomeric or enantiomeric ratio was observed. Thus, the substrate scope of **[(α-Ar*O)$_4$PcRu](CO)** was further evaluated in *t*BuOAc showing the better combination of product yield, dia- and enatioselectivity ratios at 25ºC (Table 2).

The increase of catalyst loading from 0.10 to 0.15 mol% resulted in the complete conversion of olefins. Styrene derivatives containing electron-donating substituents (*p*-Me, *m*-Me, *p*-MeO, *p*-OAc) were converted in the reactions with EDA to the corresponding substituted cyclopropanes with the similar enantiomeric excesses showing no apparent dependence on the olefin structure. The substrates bearing electron-withdrawing group (*p*-Cl, *p*-F, *p*-CN) did not show improving of the enantiomeric excesses and the reaction with *p*-vinylbenzonitrile resulted in the sharp drop of conversion. Other diazo compounds bearing electron-deficient (N_2CHR, R = CF_3, CN) and/or bulkier substituents (CO_2*t*Bu, CO_2Bn) were also amenable to react with styrene but expected increase of enantiomeric excesses was not observed. Interestingly,

Table 2. Cyclopropanation of styrene derivatives by EDA and other diazo compounds catalyzed by chiral ruthenium phthalocyanine **[(α-Ar*O)$_4$PcRu](CO)** in *tert*-butylacetate. [a]

Substrate	Diazo compound	Cat., mol.%	Cyclopropanation yields, % [b]				*ee* (*trans*), % [c]	*ee* (*cis*), % [c]
			trans	*cis*	*trans/cis*	TON		
Styrene	EDA	0.10	58	8	7.25:1	660	8	18
p-acetoxystyrene	EDA	0.10	55	15	3.67:1	700	n.d.	18
p-methylstyrene	EDA	0.15	88	12	7.3:1	750	n.d.	16
p-metoxystyrene	EDA	0.15	88	12	7.3:1	750	n.d.	15
p-fluorostyrene	EDA	0.15	58	7	8.3:1	488	n.d.	16
p-chlorostyrene	EDA	0.15	88	12	7.1:1	750	12[d]	13[d]
p-cyanostyrene	EDA	0.15	13	0	-	98	n.d.	-
m-methylstyrene	EDA	0.15	90	10	9:1	750	6	17
α-methylstyrene	EDA	0.15	20	79	4:1	743	15	8
styrene	*t*BuDA [e]	0.20 0.10	83 9	0 0	- -	623 90	18 n.d.	n.d. n.d.
styrene	BnDA [f]	0.20	43	9	4.7:1	390	n.d.	n.d.
styrene	diazoacetonitrile [g]	0.15	78 [g]	22 [g]	3.54:1	750	n.d.	8
styrene	F_3C-diazomethane [h]	0.15	34 [h]	0	-	255	4	n.d.
styrene	Me_3Si-diazomethane [i]	0.15	8 [i]	0	-	60	0	0

[a] Conditions: 0.25 mmol styrene, 0.3 mmol diazo compound (addition time: 2.5 h), 0.25 mL solvent, Ar, 25°C, reaction time: 3.5 h. [b] Yields based on olefin were determined by ^{1}H NMR. [c] Enantiomeric excesses were determined by GC-MS using a chiral column CycloSil-B. [d] Experimental error in the determination of enantiomeric excesses was bigger because of incomplete separation of the enantiomer peaks. [e] 15 % solution of N_2CHCO_2tBu in toluene was used. [f] 10 % solution of N_2CHCO_2Bn in toluene was used. [g] 0.56 M solution of N_2CHCN in 1,2-dichloroethane was used. Reaction time: 21 h. After 3.5 h: $yield_{trans}$ = 31%, $yield_{cis}$ = 7%, after 7 h: $yield_{trans}$ = 38%, $yield_{cis}$ = 17%. [h] 0.96 M solution of N_2CHCF_3 in 1,2-dichloroethane was used. Reaction time: 6h. After 3.5 h: $yield_{trans}$ = 22%. [i] Reaction temperature: 60°C, 2 M solution of $TMSCHN_2$ in hexane was used. Styrene conversion was 55%, GC-MS analysis showed the formation of several non-identified products.

3. Conclusion

In summary, two novel tetra-aryloxy-substituted ruthenium(II) phthalocyaninates with non-peripheral (α) and peripheral (β) chiral substituents based on natural (–)-menthol have been designed, synthesized and characterized. Both complexes were shown to be active in a benchmark reaction of styrene derivatives with ethyl diazoacetate in dichloromethane. Using low catalyst loading (0.1-0.15 mol%) and close to equimolecular reagent ratio at 25ºC, high yields of

cyclopropanation products with *trans*/*cis* ratios from 4.7:1 up to 5.6:1 have been obtained. The evaluation of different reaction conditions indicated a strong solvent dependence of the reaction outcome. Hence, the application of *tert*-butyl acetate significantly improved both diastereo- and enantioselectivity for the reactions catalyzed by **[(α-Ar*O)$_4$PcRu](CO)**. In contrast, these parameters were only weakly dependent on the nature of the substituents in the olefin and diazo compound.

To the best of our knowledge, we reported the first application of phthalocyanine complexes bearing chiral groups as catalysts in asymmetric carbene transfer reaction. Although the enantiomeric excesses of cyclopropyl derivatives are still modest compared with the data reported in literature for porphyrin complexes [38,52,61], this result reveals the proof of concept which can give guidelines for further optimization of the chiral phthalocyanine structure to improve the reaction diastereo- and enantioselectivity. The complex bearing *four* chiral groups at non-peripheral positions showed a better enantioselectivity in comparison with the β-substituted counterpart. To achieve a higher asymmetric induction it would be of much interest to prepare phthalocyanine bearing *eight* chiral groups *at non-peripheral positions*. In our initial effort, 3,6-difluorophthalonitrile was prepared according to the previously described protocol of selective reduction of tetrafluorophthalonitrile with $NaBH_4$ using an equivalent amount of water (see SI) [107]. However, our initial attempts to tetramerize this bulky phthalonitrile were unsuccessful (SI). Presumably, our modest result in catalysis is caused by flexibility of chiral groups and lack of strong intermolecular interactions between reagents and chiral inductor. Thus, to ensure higher enantioselectivity we envisage further preparation of phthalocyanines with either conformationally rigid chiral substituents or chiral groups capable of non-covalent interaction with substrate and reagent molecules through hydrogen bonding or π-stacking.

4. Experimental part

4.1. Materials

Unless otherwise noted, commercially available compounds including ruthenium carbonyl (Aldrich, 99%), 2,6-*bis*-(hydroxymethyl)-*p*-cresol (Aldrich, 99%), 3-nitrophthalonitrile (TCI, >98%), 4-nitrophthalonitrile (TCI, >98%), DMF (Aldrich, >99%), tetrafluorophthalonitrile (ABCR, 97%), $NaBH_4$ (Scharlau, 98%), trifluoroacetic acid (Carlo Erba and Aldrich), *o*-dichlorobenzene (99%, Sigma-Aldrich), (*1R,2S,5R*)-menthol, K_2CO_3, magnesium, hexane, ethyl

acetate, methanol were used without further purification. Pentanol (Acros Organics, 99%) was distilled and kept over Mg to remove traces of water. Chloroform was distilled and kept over $NaHCO_3$ to remove acidic impurities.

Olefins were obtained from Alfa Aesar or Sigma-Aldrich, were stored in the dark in the freezer and were used without further purification. Ethyl diazoacetatate (EDA) containing ~ 13 wt % of dichloromethane, solutions of *tert*-butyl diazoacetate (*t*BuDA, 15 wt %) and benzyl diazoacetate (BnDA, 10 wt %), in hexane, 2 M trimethylsilyldiazomethane solution in hexane were purchased from Sigma-Aldrich and stored in the dark in the freezer. The solutions of diazoacetonitrile [109] and 2,2,2-trifluorodiazoethane [110] in dichloroethane were prepared according to published protocols. The concentrations of diazo compounds were determined by ^{1}H NMR using 0.5 M DMSO solution in $CDCl_3$ as standard and solutions were stored in the dark in the freezer.

4.2. Methods

HRMS data were recorded on a Bruker QTOF Impact II mass spectrometer. MALDI TOF mass spectra were measured on a Bruker Daltonics Ultraflex mass spectrometer in positive ion mode using 2,5-dihydroxybenzoic acid (DHB) as a matrix. UV-visible absorption spectra (UV-Vis) were recorded on Thermo Evolution 210 or Agilent 8453 diade-array spectrophotometers in the 250−900 nm range in rectangular quartz with optical pathways of 10 mm. An FTIR Nexus (Nicolet) spectrophotometer with a micro-ATR accessory (Pike) was used to record IR spectra. The ^{1}H NMR spectra were acquired on a Bruker Avance HD (400 MHz) or AM 250 Bruker spectrometers at ambient temperature. The ^{1}H NMR samples were prepared in $CDCl_3$ (Cambridge Isotope Laboratories, Inc.), which was filtered through a layer of alumina prior to use. The NMR spectra were referenced to the solvent signals [111]. The reaction products were identified using the GC-MS technique (Hewlett Packard 5977B/7820A system; electron impact at 70 eV, He carrier gas, 30 m x 0.25 mm x 0.25 μm Agilent J&W CycloSil-B column).

4.3. Single-Crystal X-ray Analysis

Single crystals of phthalonitriles were obtained by slow evaporation of the corresponding solutions in mixtures of dichloromethane and heptane. The X-ray diffraction study for single crystals of **(α-Ar*O)Pn** was performed on a Bruker D8 Venture

diffractometer equipped with an area detector at 150 K using CuKα (λ = 1.54178) radiation. Absolute configuration of **(α-Ar*O)Pn** established by anomalous-dispersion effects in diffraction measurements on the crystal. XRD study for single crystals of **(β-Ar*O)Pn** was performed on a Bruker Kappa Apex II automatic four-circle diffractometer equipped with an area detector at room temperature using MoKα (λ = 0.71073) radiation. The unit cell parameters were refined over the whole dataset [112]. The experimental reflection intensities were corrected for absorption using SADABS program [113]. Using Olex2 [114], the structures were solved with the ShelXT [115] structure solution program using Intrinsic Phasing and refined by the full-matrix least-squares method (SHELXL-2014 [116]) on F^2 over the whole dataset in the anisotropic approximation for all nonhydrogen atoms. The H atoms were placed in the geometrically calculated positions with the isotropic temperature factors set at 1.2 times (CH and CH_2 groups) or 1.5 times (CH_3 group) the equivalent isotropic temperature factor of their bonded C atoms. Table S1 lists the crystallographic characteristics and details of the diffraction experiment, Tables S2-S7 list the bond lengths, angles and torsion angles. Atomic coordinates have been deposited in the Cambridge Crystallographic Data Centre (CCDC deposition codes are 2225987 for **(α-Ar*O)Pn**, 2225988 for **(β-Ar*O)Pn**) and can be obtained on request at www.ccdc.cam.ac.uk/data_request/cif

4.4. Safety note

Handling of diazo compounds should be performed in a protected well-ventilated fume cupboard. General safety precautions when using solutions of diazo compounds should be followed. It should be pointed out that neat diazo acetonitrile was reported to be explosive.[117] Consequently, these compounds should be used either in diluted solution or be generated in situ according to the published safe protocols [117]. No accidents occurred handling of diazo compounds during this study. However, the reader should be aware of the potential explosiveness and carcinogenicity of these diazo compounds. The reactions reported in the present manuscript should be not carried out without proper safety precautions and risk assessment.

4.5. Synthesis of tetra-aryloxy-substituted ruthenium phthalocyaninates containing (1R,2S,5R)-menthoxy groups

Preparation of 2,6-bis((((1R,2S,5R)-2-isopropyl-5-methylcyclohexyl)oxy)methyl)-4-methylphenol, Ar*OH.

A 100 ml single-neck flask, equipped with a magnetic stirring bar and a reflux condenser, was charged with 2,6-*bis*-(hydroxymethyl)-*p*-cresol (2.73 g, 16.3 mmol) and 15-fold excess of (–)-menthol (25.40 g, 162.8 mmol). The mixture was degassed by three-times pumping and flushing with argon on the Schlenk line and then immersed in the bath and heated at 150°C for 24 h. Unreacted menthol was removed by distillation under vacuum at 145°C. The residue was transferred onto chromatographic column packed with SiO_2 and gradient elution with a mixture of hexane/EtOAc (0 → 10 vol.%) with a control of fractions by TLC (hexane/EtOAc = 1:9, R_f = 0.68) afforded to the target product **Ar*OH** as a yellow viscous oil (3.29 g, 45%). Note 1: The distilled menthol can be involved in the same reaction repeatedly. Note 2: Since the melting point of menthol is 42.5ºC, the reaction mixture is liquid at 150ºC. Note 3: The additional chromatographic purification with SiO_2 enables to remove impurities and isolate the target phenol as a white solid. ^{1}H NMR (600 MHz, $CDCl_3$): δ 7.77 (*s*, 1H), 6.92 (*s*, 2H), 4.76 (*d*, 2H, J = 11.9 Hz), 4.50 (*d*, 2H, J = 11.9 Hz), 3.22 (*td*, 2H, J = 10.6, 4.2 Hz), 2.24 (*m*, 7H), 1.65 (*m*, 4H), 1.41 – 1.34 (*m*, 2H), 1.34 – 1.25 (*m*, 2H), 1.03 – 0.84 (*m*, 18H), 0.75 (*d*, 6H, J = 6.9 Hz). ^{13}C{^{1}H} NMR (151 MHz, $CDCl_3$): δ 151.75, 128.56, 128.31, 124.42, 79.53, 67.70, 48.45, 40.38, 34.70, 31.76, 25.75, 23.41, 22.46, 21.20, 20.66, 16.19. HR MS (ESI, *m/z*): calcd for $C_{29}H_{48}O_3^+$ $[M+H]^+$, 445.3676; found, 445.3679. IR, cm^{-1}: 264, 302, 344, 406, 448, 466, 510, 548, 559, 594, 619, 639, 711, 742, 783, 847, 863, 910, 920, 942, 973, 1010, 1055, 1083, 1102, 1152, 1180, 1226, 1262, 1342, 1367, 1386, 1450, 1482, 2844, 2869, 2914, 2950, 3309 (ν^{OH}). M.p. = 67-69ºC.

Preparation of 3-(2,6-bis((((1R,2S,5R)-2-isopropyl-5-methylcyclohexyl)oxy)methyl)-4-methylphenoxy)phthalonitrile, (α-Ar*O)Pn.

A 100 ml single-neck flask, equipped with a magnetic stirring bar and a reflux condenser, was charged with phenol Ar*OH (1.66 g, 3.74 mmol), 3-nitrophthalonitrile (0.54 g, 3.12 mmol) and potassium carbonate (2.58 g, 18.7 mmol). DMF (12 mL) was added under vacuum and the suspension was degassed by three-times pumping and flushing with argon on the Schlenk line, immersed in the bath and heated at 80°C for 24 h. Then, the reaction mixture was extracted with a mixture of saturated NaCl aqueous solution (50 ml) and ethylacetate (4 x 15 ml). Organic phases were combined and evaporated. The residue was transferred onto chromatographic col-

umn packed with SiO_2 and gradient elution with a mixture of hexane/EtOAc (0 → 10 vol.%) with a control of fractions by TLC (hexane/EtOAc = 2:8, R_f = 0.68) afforded to the target phthalonitrile **(α-Ar*O)Pn** as a beige crystals (1.10 g, 60%). ^{1}H NMR (600 MHz, $CDCl_3$): δ 7.43 (*m*, 1H), 7.39 (*m*, 1H), 7.29 (*m*, 2H), 6.84 (*m*, 1H), 4.47 (*m*, 2H), 4.27 – 4.15 (*m*, 2H), 3.02 (m, 2H), 2.39 (*s*, 3H), 2.12 – 2.01 (*m*, 2H), 1.89 – 1.74 (*m*, 2H), 1.61 (*m*, 2H), 1.55 (*m*, 2H), 1.35 – 1.21 (*m*, 2H), 1.15 – 0.30 (*m*, 26H). ^{13}C{^{1}H} NMR (151 MHz, $CDCl_3$): δ 161.88, 146.27, 137.20, 134.10, 131.65, 131.14, 126.24, 119.72, 116.85, 115.36, 112.79, 104.30, 79.40, 79.09, 64.86, 48.41, 48.30, 34.59, 31.69, 31.46, 25.75, 25.49, 23.38, 23.25, 22.42, 21.18, 21.11, 16.34, 16.07. HR MS (ESI, *m/z*): calcd for $C_{37}H_{50}N_2O_3^+$ $[M+H]^+$, 571.3894; found, 571.3891. IR, cm^{-1}: 454, 533, 551, 572, 606, 728, 796, 846, 862, 918, 983, 1024, 1042, 1086, 1113, 1138, 1189, 1262, 1310, 1341, 1367, 1384, 1456, 1577, 2332 (ν^{CN}), 2864, 2919, 2952. M.p. = 123-125ºC.

Preparation of 4-(2,6-bis((((1R,2S,5R)-2-isopropyl-5-methylcyclohexyl)oxy)methyl)-4-methylphenoxy)phthalonitrile, (β-Ar*O)Pn.

A 100 ml single-neck flask, equipped with a magnetic stirring bar and a reflux condenser, was charged with phenol Ar*OH (0.567 g, 1.27 mmol), 4-nitrophthalonitrile (0.147 g, 0.85 mmol), potassium carbonate (0.703 g, 5.1 mmol) and DMF (10 mL). The suspension was de-gassed by three-times pumping and flushing with argon on the Schlenk line, immersed in the bath and heated at 80°C for 24 h. The reaction mixture was extracted with a mixture of saturated NaCl aqueous solution (50 mL) and ethylacetate (5 x 10 mL). Organic phases were combined and evaporated. The residue was transferred onto chromatographic column packed with SiO_2 and gradient elution with a mixture of hexane/EtOAc (0 → 10 vol.%) with a control of fractions by TLC (hexane/EtOAc = 1:9, R_f = 0.42) afforded the oil which was dissolved in hexane at 60°C, cooled in a freezer and precipitate was separated by filtration. The mother liquid was evaporated with a formation of target phthalonitrile **(β-Ar*O)Pn** as a beige crystals (282 mg, 59%). ^{1}H NMR (600 MHz, $CDCl_3$): δ 7.66 (*d*, 1H, J = 8.7 Hz), 7.29 (*s*, 2H), 7.17 (*d*, 1H, J = 2.5 Hz), 7.11 (*dd*, 1H, J = 8.7, 2.5 Hz), 4.44 – 4.38 (*d*, 2H, J = 11.2 Hz), 4.17 – 4.11 (*d*, 2H, J = 11.1 Hz), 3.04 – 2.96 (*td*, 2H, J = 10.6, 4.1 Hz), 2.40 (*s*, 3H), 2.02 – 1.94 (*m*, 2H), 1.91 (*m*, 2H), 1.62 (*m*, 2H), 1.57 (*m*, 2H), 1.32 – 1.21 (*m*, 2H), 1.15 – 1.05 (*m*, 2H), 0.94 – 0.73 (*m*, 16H), 0.69 – 0.62 (*m*, 8H). ^{13}C{^{1}H} NMR (151 MHz, $CDCl_3$): δ 162.46, 146.28, 137.16, 135.23, 131.53, 131.32, 120.64, 120.26, 117.58, 115.57, 115.07, 108.38, 79.30, 64.93, 48.34, 40.20, 34.56, 31.62, 25.65, 23.34, 22.45, 21.18, 21.10, 16.25. HR MS (ESI, *m/z*): calcd for $C_{37}H_{50}N_2O_3^+$

$[M+H]^+$, 571.3894; found, 571.3890. IR, cm^{-1}: 340, 523, 593, 632, 729, 775, 820, 843, 869, 919, 950, 992, 1008, 1055, 1066, 1085, 1110, 1136, 1160, 1194, 1242, 1277, 1315, 1366, 1384, 1471, 1592, 2230 (ν^{CN}), 2864, 2920, 2947. M.p. = 119-121ºC.

Preparation of 3,6-difluorophthalonitrile.

A 100 ml double-neck flask, equipped with a magnetic stirring bar and a reflux condenser, was charged with $NaBH_4$ (451 mg, 11.87 mmol) and immersed in an ice-cold bath at 6-7°C. Then, under argon sodium borohydride was dissolved in 10 ml of dry THF and 214 μl (11.87 mmol) of water was poured. Next, 20 ml of solution tetrafluoronitrile (1.08 g, 5.40 mmol) in THF was added. Within 30 min, reaction mass changed color to dark-purple. After 3 h, stirring was stopped and solvent was evaporated under reduced pressure. The residue was transferred onto chromatographic column packed with SiO_2 and gradient elution with a mixture of $CHCl_3$ + 0 → 4 vol.% methanol with a control of fractions by TLC (hexane/acetone = 1:1, R_f = 0.87) afforded the target 3,6-difluorophthalonitrile as a beige powder (312 mg, 35%). ^1H and ^{19}F NMR spectrum coincided with those previously described [107]. ^1H NMR (300 MHz, acetone-d_6): δ 7.99 – 7.94 (m, 2H). ^{19}F NMR (282 MHz, acetone-d_6) δ -110.26 (s, 2F). IR, cm^{-1}: 369, 437, 452, 504, 621, 626, 734, 808, 846, 924, 1096, 1152, 1231, 1258, 1362, 1477, 1608, 2243 (ν^{CN}), 2867, 2922, 2954, 3076.

Note: in the previously published results 3,6-difluoronitrile described as «poorly stored»[107]. Nevertheless, according to ^1H and ^{19}F NMR spectra, no evidence of degradation was detected after one month of storage at room temperature.

Preparation of 3,6-bis(2,6-bis((((1R,2S,5R)-2-isopropyl-5-methylcyclohexyl)oxy)methyl)-4-methylphenoxy)phthalonitrile, (α-Ar*O)$_2$Pn.

A 100 ml double-neck flask, equipped with a round magnetic stirring bar and a reflux condenser, was charged with 3,6-difluorophthalonitrile (87 mg, 0.53 mmol), the phenol Ar*OH (1.180 g, 2.65 mmol) and K_2CO_3 (734 mg, 5.31 mmol). 10 ml of dry DMSO was poured under vacuo and the suspension was degassed by three-times pumping and flushing with argon on the Schlenk line, immersed in the bath and heated at 80°C. After 3 h 10 min, according to TLC, full conversion of 3,6-difluorophthalonitrile was accomplished and reaction was stopped. After cooling to ambient temperature, reaction mass was poured in 100 ml of water and extracted with EtOAc (3 x 100 ml) with aim to remove DMSO. Combined organic phase was evaporated and the residue was transferred onto chromatographic column packed with SiO_2. Gradient elution

with a mixture of hexane/EtOAc (0 → 10 vol.%) with a control of fractions by TLC (hexane/acetone = 8:2, R_f = 0.65) afforded to the target phthalonitrile **(α-Ar*O)$_2$Pn** as beige crystals (500 mg, 93%). ^{1}H NMR (600 MHz, Acetone) δ 7.34 (*s*, 2H), 6.74 (*s*, 1H), 4.55 (*d*, *J* = 11.5 Hz, 2H), 4.28 (*d*, *J* = 11.5 Hz, 2H), 3.12 (*td*, *J* = 10.4, 4.1 Hz, 2H), 2.36 (*s*, 3H), 2.18 – 2.08 (*m*, 5H), 1.67 – 1.58 (*m*, 4H), 1.35 (*s*, 2H), 1.03 – 0.70 (*m*, 22H), 0.69 (*d*, *J* = 7.0 Hz, 6H). ^{13}C{^{1}H} NMR (151 MHz, $CDCl_3$): *δ* 155.67, 145.94, 136.78, 131.65, 130.17, 119.96, 112.48, 104.19, 79.25, 64.43, 48.31, 40.17, 34.55, 31.47, 25.59, 23.28, 22.33, 21.07, 21.02, 16.18. IR, cm^{-1}: 456,507, 569, 818, 846, 865, 919, 947, 1012, 1083, 1109, 1138, 1190, 1256, 1342, 1367, 1459, 1703, 2232 (ν^{CN}), 2866, 2918, 2952.

Preparation of 1(4),8(11),15(18),22(25)-tetrakis(2,6-bis((((1R,2S,5R)-2-isopropyl-5-methylcyclohexyl)oxy)methyl)-4-methylphenoxy)-phthalocyanine, H$_2$[(α-Ar*O)$_4$Pc].

A 25 ml double-neck flask, equipped with a magnetic stirring bar and a reflux condenser, was charged with phthalonitrile (α-Ar*O)Pn (234 mg, 0.42 mmol) and metallic magnesium (47 mg, 2.10 mmol). Under vacuum, 3 mL of dry pentanol was added, the suspension degassed by three-times pumping and flushing with argon on the Schlenk line, immersed in the bath and heated at 155°C for 17 h. The formation of Mg(II) complex was confirmed by UV-Vis and MALDI-TOF mass-spectra of reaction mixture samples (UV-Vis in $CHCl_3$, λ_{max}/nm ($A_{norm.}$): 704 (1.00), 635 (0.18), 371 (0.25), 324 (0.23). MALDI TOF MS, m/z: found 2306.6 for $[M]^+$, calculated for $[C_{148}H_{200}MgN_8O_{12}]^+$ – 2306.5). Then the solvent was removed under reduced pressure; the residue was dissolved in 10 mL of chloroform. Under reflux conditions, 1 mL of aqueous solution of trifluoroacetic acid (50 vol. %) was added. The UV/Vis spectra showed disappearance of Q-band of magnesium complex at 704 nm within 5 min and appearance of Q-bands of the metal-free phthalocyanine at 727 and 694 nm. The reaction mixture was cooled to ambient temperature, diluted with water, neutralized with $NaHCO_3$, extracted with chloroform and then solvents were evaporated. The green residue was purified by column chromatography on Al_2O_3 with gradient elution with $CHCl_3$ + 50 → 0 vol. % hexane and with $CHCl_3$ + 0 → 10 vol.% methanol. Further purification by size-exclusion chromatography on Bio-Beads SX-1 gel in $CHCl_3$ + 2.5 vol.% MeOH, afforded the pure phthalocyanine **H$_2$[(α-Ar*O)$_4$Pc]** as a dark-green solid (142 mg, 59%). UV-Vis in CH_2Cl_2, λ_{max}/nm (lgε): 725 (5.16), 693 (5.10), 661 (4.57), 627 (4.45), 317 (4.69). ^{1}H NMR (600 MHz, $CDCl_3$): *δ* 9.27 – 9.01 (*m*, 4H), 8.09 – 7.81 (*m*, 4H), 7.63 – 7.27 (*m*, 8H), 7.24 – 7.12 (*m*, 4H), 5.14 – 4.10 (*m*, 16H). 3.07 – 2.72 (*m*, 8H),

2.47 – 0.02 (*m*, 158H). MS (MALDI TOF, *m/z*): calcd for $C_{148}H_{202}N_8O_{12}^+$ $[M]^+$, 2284.5; found, 2284.0. IR, cm^{-1}: 667, 754, 803, 848, 866, 920, 940, 1020, 1053, 1069, 1106, 1134, 1195, 1224, 1247, 1312, 1334, 1367, 1467, 1593, 2866, 2918, 2952, 3297 (ν^{NH}).

Preparation of 2(3),9(10),16(17),23(24)-tetrakis(2,6-bis((((1R,2S,5R)-2-isopropyl-5-methylcyclohexyl)oxy)methyl)-4-methylphenoxy)-phthalocyanine, $H_2[(\beta\text{-}Ar^*O)_4Pc]$.

A 25 ml double-neck flask, equipped with a magnetic stirring bar and a reflux condenser, was charged with phthalonitrile (β-Ar*O)Pn (200 mg, 0.35 mmol) and metallic magnesium (17 mg, 0.70 mmol). After addition of 5 mL of dry pentanol, the suspension was degassed by three-times pumping and flushing with argon on the Schlenk line and was heated at 155°C for 17 h. The formation of Mg(II) complex was confirmed by UV-Vis and MALDI-TOF mass-spectra of reaction mixture samples (UV-Vis in $CHCl_3$, λ_{max}/nm ($A_{norm.}$): 681 (1.00), 619 (0.19), 353 (0.51), 280 (0.26). MS (MALDI TOF, *m/z*): calcd for $C_{148}H_{200}MgN_8O_{12}^+$ $[M]^+$, 2306.5; found, 2306.8). The reaction mixture was dried by evaporation of solvent and crude residue was transferred onto column, packed with Al_2O_3. Gradient elution with $CHCl_3$ + 80 → 0 vol. % hexane and with $CHCl_3$ + 0 → 5 vol.% methanol gave the magnesium complex which was purified by size-exclusion chromatography on Bio-Beads SX-1 gel in $CHCl_3$ + 2.5 vol.% MeOH, affording pure compound **Mg[(α-Ar*O)$_4$Pc]** as a dark-green solid (123 mg, 61%). Then, magnesium phthalocyaninate was dissolved in 15 mL $CHCl_3$ and 1 mL aqueous solution of trifluoroacetic acid (50 vol. %) was added. UV/Vis spectra showed disappearance of the Q-band of the magnesium complex at 681 nm within 1 min and appearance of Q-bands of the metal free phthalocyanine at 707 and 671 nm. The reaction mixture was neutralized with $NaHCO_3$, extracted with chloroform and then solvents were evaporated. The target metal free phthalocyanine **H$_2$[(β-Ar*O)$_4$Pc]** was isolated quantitatively after evaporation of solvents. UV-Vis in CH_2Cl_2, λ_{max}/nm (lgε): 705 (5.16), 670 (5.08), 641 (4.63), 608 (4.44), 343 (4.83), 289 (4.60). ^{1}H NMR (600 MHz, $CDCl_3$): δ 9.40 – 9.25 (*m*, 4H), 8.84 – 8.76 (*m*, 4H), 7.73 – 7.58 (*m*, 4H), 7.51 – 7.50 (*m*, 8H), 4.75 – 4.71 (*d*, 8H, J = 12.2 Hz), 4.57 – 4.54 (*d*, 8H, J = 12.3 Hz), 3.14 – 3.10 (*td*, 8H, J = 10.6, 3.5 Hz), 2.57 – 2.55 (*s*, 12H), 2.31 – 2.25 (*m*, 8H), 2.06 – 2.01 (*m*, 8H), 1.52 – 1.40 (*m*, 20H), 1.26 – 1.13 (*m*, 20H), 0.80 – 0.61 (*m*, 88H), -0.16 – -0.28 (*m*, 2H). IR, cm^{-1}: 703, 753, 822, 847, 867, 922, 1007, 1066, 1092, 1111, 1221, 1252, 1321, 1340, 1369, 1394, 1425, 1459, 1499, 1615, 2867, 2918, 2952, 3295 (ν^{NH}).

Preparation of 1(4),8(11),15(18),22(25)-tetrakis(2,6-bis((((1R,2S,5R)-2-isopropyl-5-methylcyclohexyl)oxy)methyl)-4-methylphenoxy)-phthalocyaninatoruthenium(II) carbonyl, [(α-Ar*O)$_4$PcRu](CO).

A 25 ml double-neck flask, equipped with a magnetic stirring bar and a reflux condenser, was charged with phthalocyanine **H$_2$[(α-Ar*O)$_4$Pc]** (31.0 mg, 13.9 μmol), $Ru_3(CO)_{12}$ (13.3 mg, 20.9 μmol) and 3 mL of *o*-DCB. The suspension was degassed by three-times pumping and flushing with argon on the Schlenk line and was heated to 190°C. Under argon stream, another portion of $Ru_3(CO)_{12}$ (11 mg,17.2 μmol) was added after 30 min. Reaction mixture was refluxed for 1h until Q-bands of the starting ligand at 727 and 694 nm disappeared and Q-band of the metal complex at 673 nm appeared. The reaction mixture was transferred onto column packed with SiO_2. Gradient elution with $CHCl_3$ + 50 → 0 vol. % hexane and with $CHCl_3$ + 0 → 10 vol.% methanol afforded the blue fractions containing the target complex as a major product. Subsequent purification by size-exclusion chromatography on Bio-Beads SX-1 gel in $CHCl_3$ + 2.5 vol.% MeOH gave the pure ruthenium complex **[(α-Ar*O)$_4$PcRu](CO)** as a dark-blue solid (12 mg, 37%). UV-Vis in CH_2Cl_2, λ_{max}/nm (lgε): 675 (5.32), 607 (4.67), 349 (4.51), 295 (4.96). ^{1}H NMR (600 MHz, $CDCl_3$): *δ* 9.08 – 8.85 (*m*, 4H), 7.82 – 7.66 (*m*, 4H), 7.58 – 7.49 (*m*, 4H), 7.21 – 7.04 (*m*, 8H), 5.46 – 3.66 (*m*, 16H), 3.21 – -0.13 (*m*, 164H). HR MS (ESI, *m/z*): calcd for $C_{148}H_{201}N_8O_{13}Ru^+$ $[M+H]^+$, 2412.4393;found, 2412.4324.

Preparation of 2(3),9(10),16(17),23(24)-tetrakis(2,6-bis((((1R,2S,5R)-2-isopropyl-5-methylcyclohexyl)oxy)methyl)-4-methylphenoxy)- phthalocyaninatoruthenium(II) carbonyl, [(β-Ar*O)$_4$PcRu](CO).

A 25 mL double-neck flask, equipped with a magnetic stirring bar and a reflux condenser, was charged with phthalocyanine **H$_2$[(β-Ar*O)$_4$Pc]** (81.2 mg, 36.1 μmol), $Ru_3(CO)_{12}$ (34.6 mg, 54.1 μmol) and 5 mL of *o*-DCB. The suspension was degassed by three-times pumping and flushing with argon on the Schlenk line and heated to 190°C. Under argon stream another portion of $Ru_3(CO)_{12}$ (17 mg, 26.6 μmol) was added after 15 min. The reaction mixture was refluxed for 1h until disappearance of the Q-bands of the starting ligand at 701 and 671 nm and appearance of the Q-band of the metal complex at 659 nm. The reaction mixture was transferred onto column packed with SiO_2. Gradient elution with $CHCl_3$ + 50 → 0 vol. % hexane and with $CHCl_3$ + 0 → 10 vol.% methanol afforded the blue fractions containing target complex as a major product. Subsequent purification by column chromatography on Al_2O_3 with gradient elution

with $CHCl_3$ + 20 → 0 vol. % hexane and with $CHCl_3$ + 0 → 8 vol.% methanol gave the pure ruthenium complex **[(β-Ar*O)$_4$PcRu](CO)** as a dark-blue solid (23 mg, 26%). UV-Vis in $CHCl_3$, λ_{max}, nm ($A_{norm.}$): 659 (1.00), 595 (0.22), 305 (0.61). ^{1}H NMR (300 MHz, $CDCl_3$): δ 9.21 – 9.04 (*m*, 4H), 8.76 – 8.60 (*m*, 4H), 7.52 – 7.41 (*m*, 8H), 7.20 – 7.06 (*m*, 4H), 4.77 – 4.34 (*m*, 16H), 3.23 – 0.88 (*m*, 164H). HR MS (ESI, *m/z*): calcd for $C_{148}H_{201}N_8O_{13}Ru^+$ $[M+H]^+$, 2412.4393; found, 2412.4370. IR, cm^{-1}: 383, 440, 526, 593, 666, 749, 823, 846, 868, 920, 955, 1009, 1049, 1083, 1101, 1215, 1328, 1367, 1396, 1455, 1611, 1651, 1962 (ν^{CO}), 2866, 2919, 2952.

4.6. Catalysis

Cyclopropanation of alkenes catalyzed by ruthenium phthalocyanines bearing chiral substituents [(α- or β-Ar*O)$_4$PcRu](CO).

Typical procedure: A 2mM solution of ruthenium complex (125-250 μL for 2.5-5□10^{-4} mmol, 0.10-0.20 mol.%) in dichloromethane (purified by filtration through alumina prior to use) was placed in a 1 mL vial and was dried under stream of Ar. Then, 0.25 mL of *tert*-butyl acetate solvent was added followed by addition of alkene (0.25 mmol, 1M, 1 eq.). The solution was bubbled with a stream of argon for 1-2 min and 1.1 eq. of diazo compound was slowly added during 2.5 h by a syringe pump (EDA – 2 M in *tert*-butyl acetate; N_2CHCN – 0.56 M in $C_2H_4Cl_2$; CF_3CHN_2 – 0.94 M in $C_2H_4Cl_2$; N_2CHTMS – 2 M in hexane; N_2CHCO_2tBu – 15 % solution in toluene; N_2CHCO_2Bn – 10 % solution in toluene). The reaction mixtures were analyzed by GC-MS after 3 h and by ^{1}H NMR after 3.5 h. Substrate conversion and a *trans*/*cis* ratio of the obtained cyclopropanes were determined from ^{1}H NMR data and enantimeric excesses (*ee*) were calculated from GC-MS data. The spectral characteristics for the reaction products were identical to those previously reported.

CRediT authorship contribution statement

Andrey P. Kroitor: Investigation, Visualization, Writing - Review & Editing, Funding acquisition. **Anna A. Sinelshchikova**: Investigation. **Mikhail S. Grigoriev**: Investigation. **Gayane A. Kirakosyan**: Investigation. **Alexander G. Martynov**: Conceptualization, Visualization, Writing - Review & Editing, Funding acquisition. **Yulia G. Gorbunova**: Supervision, Project administration. **Alexander B. Sorokin**: Supervision, Project administration.

Declaration of competing interest

The authors declare that they have no known competing financial interests or personal relationships that could have appeared to influence the work reported in this paper.

Data availability

Data will be made available on request.

Author information

Corresponding Author

*E-mail for **Alexander G. Martynov** - martynov@phyche.ac.ru; **Yulia G. Gorbunova** - yulia@igic.ras.ru; **Alexander B. Sorokin** - alexander.sorokin@ircelyon.univ-lyon1.fr.

Acknowledgment

Synthesis and characterisation of ruthenium phthalocyanines **[(α- or β-Ar*O)$_4$PcRu](CO).** their precursors and all catalytic tests were supported by CNRS and RFBR through International Emerging Action 2021 and research project 21-53-15004. Synthesis and characterisation of nitrile **[(α-Ar*O)$_2$Pn** and their precursor were supported by RSF research project 23-73-01126. X-ray diffraction measurements were performed using equipment of the Shared Facility Centers of the Frumkin Institute of Physical Chemistry and Electrochemistry, RAS (CKP FMI IPCE RAS) and Kurnakov Institute of General and Inorganic chemistry, RAS.

Associated content

Supporting Information

Characterization of compounds and reaction products - Fig. S1-S... Additional XRD data – Tables S1-S7.

References

[1] Beletskaya IP, Nájera C, Yus M. Stereodivergent Catalysis. Chem Rev 2018;118:5080–200. https://doi.org/10.1021/acs.chemrev.7b00561.

[2] Beletskaya IP, Nájera C, Yus M. Chemodivergent reactions. Chem Soc Rev 2020;49:7101–66. https://doi.org/10.1039/d0cs00125b.

[3] Cussó O, Ribas X, Costas M. Biologically inspired non-heme iron-catalysts for asymmetric epoxidation; Design principles and perspectives. Chem Commun 2015;51:14285–98. https://doi.org/10.1039/c5cc05576h.

[4] Olivo G, Cussó O, Borrell M, Costas M. Oxidation of alkane and alkene moieties with biologically inspired nonheme iron catalysts and hydrogen peroxide: from free radicals to stereoselective transformations. J Biol Inorg Chem 2017;22:425–52.

https://doi.org/10.1007/s00775-016-1434-z.
[5] Talsi EP, Bryliakov KP. Chemo- and stereoselective CH oxidations and epoxidations/cis-dihydroxylations with H2O2, catalyzed by non-heme iron and manganese complexes. Coord Chem Rev 2012;256:1418–34. https://doi.org/10.1016/j.ccr.2012.04.005.
[6] Milan M, Bietti M, Costas M. Enantioselective aliphatic C-H bond oxidation catalyzed by bioinspired complexes. Chem Commun 2018;54:9559–70. https://doi.org/10.1039/c8cc03165g.
[7] Newton CG, Wang SG, Oliveira CC, Cramer N. Catalytic Enantioselective Transformations Involving C-H Bond Cleavage by Transition-Metal Complexes. Chem Rev 2017;117:8908–76. https://doi.org/10.1021/acs.chemrev.6b00692.
[8] Intrieri D, Carminati DM, Gallo E. Recent Advances in Metal Porphyrinoid-Catalyzed Nitrene and Carbene Transfer Reactions, 2016, p. 1–99. https://doi.org/10.1142/9789813149588_0001.
[9] Intrieri D, Carminati DM, Gallo E. The ligand influence in stereoselective carbene transfer reactions promoted by chiral metal porphyrin catalysts. Dalt Trans 2016;45:15746–61. https://doi.org/10.1039/C6DT02094A.
[10] Damiano C, Sonzini P, Gallo E. Iron catalysts with N-ligands for carbene transfer of diazo reagents. Chem Soc Rev 2020;49:4867–905. https://doi.org/10.1039/d0cs00221f.
[11] Titanyuk ID, Beletskaya IP, Peregudov AS, Osipov SN. Trifluoromethylated cyclopropanes and epoxides from CuI-mediated transformations of α-trifluoromethyl-diazophosphonate. J Fluor Chem 2007;128:723–8. https://doi.org/10.1016/j.jfluchem.2007.02.003.
[12] Simonneaux G, Le Maux P, Ferrand Y, Rault-Berthelot J. Asymmetric heterogeneous catalysis by metalloporphyrins. Coord Chem Rev 2006;250:2212–21. https://doi.org/10.1016/j.ccr.2006.01.014.
[13] Lu H, Zhang XP. Catalytic C–H functionalization by metalloporphyrins: recent developments and future directions. Chem Soc Rev 2011;40:1899–909. https://doi.org/10.1039/C0CS00070A.
[14] Gross Z, Ini S. Asymmetric Catalysis by a Chiral Ruthenium Porphyrin: Epoxidation, Hydroxylation, and Partial Kinetic Resolution of Hydrocarbons. Org Lett 1999;1:2077–80. https://doi.org/10.1021/ol991131b.
[15] Zhang R, Yu WY, Che CM. Catalytic enantioselective oxidation of aromatic hydrocarbons with D 4-symmetric chiral ruthenium porphyrin catalysts. Tetrahedron Asymmetry 2005;16:3520–6. https://doi.org/10.1016/j.tetasy.2005.08.059.
[16] Zhang R, Yu W-Y, Lai T-S, Che C-M. Enantioselective hydroxylation of benzylic C–H bonds by D4-symmetric chiral oxoruthenium porphyrins†. Chem Commun 1999:1791–2. https://doi.org/10.1039/a904100a.
[17] Xu X, Wang Y, Cui X, Wojtas L, Zhang XP. Metalloradical activation of α-formyldiazoacetates for the catalytic asymmetric radical cyclopropanation of alkenes. Chem Sci 2017;8:4347–51. https://doi.org/10.1039/C7SC00658F.
[18] Wang Y, Wen X, Cui X, Wojtas L, Zhang XP. Asymmetric Radical Cyclopropanation of Alkenes with In Situ-Generated Donor-Substituted Diazo Reagents via Co(II)-Based Metalloradical Catalysis. J Am Chem Soc 2017;139:1049–52. https://doi.org/10.1021/jacs.6b11336.
[19] Carminati DM, Intrieri D, Caselli A, Le Gac S, Boitrel B, Toma L, et al. Designing 'Totem' C 2 -Symmetrical Iron Porphyrin Catalysts for Stereoselective Cyclopropanations. Chem - A Eur J 2016;22:13599–612.

https://doi.org/10.1002/chem.201602289.
[20] Talele TT. The “Cyclopropyl Fragment” is a Versatile Player that Frequently Appears in Preclinical/Clinical Drug Molecules. J Med Chem 2016;59:8712–56. https://doi.org/10.1021/acs.jmedchem.6b00472.
[21] Brandenberg OF, Fasan R, Arnold FH. Exploiting and engineering hemoproteins for abiological carbene and nitrene transfer reactions. Curr Opin Biotechnol 2017;47:102–11. https://doi.org/10.1016/j.copbio.2017.06.005.
[22] Wittmann BJ, Knight AM, Hofstra JL, Reisman SE, Jennifer Kan SB, Arnold FH. Diversity-Oriented Enzymatic Synthesis of Cyclopropane Building Blocks. ACS Catal 2020;10:7112–6. https://doi.org/10.1021/acscatal.0c01888.
[23] Liu Z, Arnold FH. New-to-nature chemistry from old protein machinery: carbene and nitrene transferases. Curr Opin Biotechnol 2021;69:43–51. https://doi.org/10.1016/j.copbio.2020.12.005.
[24] Lebel H, Marcoux J-F, Molinaro C, Charette AB. Stereoselective Cyclopropanation Reactions. Chem Rev 2003;103:977–1050. https://doi.org/10.1021/cr010007e.
[25] Tinoco A, Wei Y, Bacik J-P, Carminati DM, Moore EJ, Ando N, et al. Origin of High Stereocontrol in Olefin Cyclopropanation Catalyzed by an Engineered Carbene Transferase. ACS Catal 2019;9:1514–24. https://doi.org/10.1021/acscatal.8b04073.
[26] Carminati DM, Fasan R. Stereoselective Cyclopropanation of Electron-Deficient Olefins with a Cofactor Redesigned Carbene Transferase Featuring Radical Reactivity. ACS Catal 2019;9:9683–97. https://doi.org/10.1021/acscatal.9b02272.
[27] Dydio P, Key HM, Nazarenko A, Rha JY-E, Seyedkazemi V, Clark DS, et al. An artificial metalloenzyme with the kinetics of native enzymes. Science (80-) 2016;354:102–6. https://doi.org/10.1126/science.aah4427.
[28] Gu Y, Natoli SN, Liu Z, Clark DS, Hartwig JF. Site- Selective Functionalization of (sp 3)C−H Bonds Catalyzed by Artificial Metalloenzymes Containing an Iridium- Porphyrin Cofactor. Angew Chemie Int Ed 2019;58:13954–60. https://doi.org/10.1002/anie.201907460.
[29] Oohora K, Hayashi T. Myoglobins engineered with artificial cofactors serve as artificial metalloenzymes and models of natural enzymes. Dalt Trans 2021;50:1940–9. https://doi.org/10.1039/D0DT03597A.
[30] Key HM, Dydio P, Liu Z, Rha JYE, Nazarenko A, Seyedkazemi V, et al. Beyond Iron: Iridium-Containing P450 Enzymes for Selective Cyclopropanations of Structurally Diverse Alkenes. ACS Cent Sci 2017;3:302–8. https://doi.org/10.1021/acscentsci.6b00391.
[31] Zhu S, Zhou Q. Iron-catalyzed transformations of diazo compounds. Natl Sci Rev 2014;1:580–603. https://doi.org/10.1093/nsr/nwu019.
[32] Le Maux P, Nicolas I, Chevance S, Simonneaux G. Chemical reactivity of 6-diazo-5-oxo-l-norleucine (DON) catalyzed by metalloporphyrins (Fe,Ru). Tetrahedron 2010;66:4462–8. https://doi.org/10.1016/j.tet.2010.04.080.
[33] Du G, Andrioletti B, Rose E, Woo LK. Asymmetric Cyclopropanation of Styrene Catalyzed by Chiral Macrocyclic Iron(II) Complexes. Organometallics 2002;21:4490–5. https://doi.org/10.1021/om0204641.
[34] Lai T, Chan F, So P, Ma D, Wong K, Che C. Alkene cyclopropanation catalyzed by Halterman iron porphyrin: participation of organic bases as axial ligands. Dalt Trans 2006:4845–51. https://doi.org/10.1039/b606757c.
[35] Intrieri D, Le Gac S, Caselli A, Rose E, Boitrel B, Gallo E. Highly diastereoselective

cyclopropanation of α-methylstyrene catalysed by a C2 -symmetrical chiral iron porphyrin complex. Chem Commun 2014;50:1811–3. https://doi.org/10.1039/C3CC48605B.
[36] Rioz-Martínez A, Oelerich J, Ségaud N, Roelfes G. DNA-Accelerated Catalysis of Carbene-Transfer Reactions by a DNA/Cationic Iron Porphyrin Hybrid. Angew Chemie Int Ed 2016;55:14136–40. https://doi.org/10.1002/anie.201608121.
[37] Le Maux P, Juillard S, Simonneaux G. Asymmetric Synthesis of Trifluoromethylphenyl Cyclopropanes Catalyzed by Chiral Metalloporphyrins. Synthesis (Stuttg) 2006;2006:1701–4. https://doi.org/10.1055/s-2006-926451.
[38] Nicolas I, Maux P Le, Simonneaux G. Synthesis of chiral water-soluble metalloporphyrins (Fe, Ru,): new catalysts for asymmetric carbene transfer in water. Tetrahedron Lett 2008;49:5793–5. https://doi.org/10.1016/j.tetlet.2008.07.133.
[39] Nicolas I, Roisnel T, Maux P Le, Simonneaux G. Asymmetric intermolecular cyclopropanation of alkenes by diazoketones catalyzed by Halterman iron porphyrins. Tetrahedron Lett 2009;50:5149–51. https://doi.org/10.1016/j.tetlet.2009.06.131.
[40] Ferrand Y, Le Maux P, Simonneaux G. Macroporous chiral ruthenium porphyrin polymers: a new solid-phase material used as a device for catalytic asymmetric carbene transfer. Tetrahedron: Asymmetry 2005;16:3829–36. https://doi.org/10.1016/j.tetasy.2005.10.021.
[41] Ferrand Y, Poriel C, Le Maux P, Rault-Berthelot J, Simonneaux G. Asymmetric heterogeneous carbene transfer catalyzed by optically active ruthenium spirobifluorenylporphyrin polymers. Tetrahedron: Asymmetry 2005;16:1463–72. https://doi.org/10.1016/j.tetasy.2005.01.051.
[42] Nicolas I, Maux P Le, Simonneaux G. Intermolecular asymmetric cyclopropanation with diazoketones catalyzed by chiral ruthenium porphyrins. Tetrahedron Lett 2008;49:2111–3. https://doi.org/10.1016/j.tetlet.2008.01.129.
[43] Zhou C-Y, Huang J-S, Che C-M. Ruthenium-Porphyrin-Catalyzed Carbenoid Transfer Reactions. Synlett 2010;2010:2681–700. https://doi.org/10.1055/s-0030-1259017.
[44] Raoul N, Gallo E, Rose E. Synthesis of chiral ruthenium and cobalt (meso-2-amidophenyl)porphyrins and their catalytic activity in cyclopropanation reactions. J Porphyr Phthalocyanines 2011;15:602–11. https://doi.org/10.1142/S1088424611003525.
[45] Chan K-H, Guan X, Lo VK-Y, Che C-M. Elevated Catalytic Activity of Ruthenium(II)-Porphyrin-Catalyzed Carbene/Nitrene Transfer and Insertion Reactions with N-Heterocyclic Carbene Ligands. Angew Chemie Int Ed 2014;53:2982–7. https://doi.org/10.1002/anie.201309888.
[46] Simonneaux G, Srour H, Maux P, Chevance S, Carrie D. Metalloporphyrin Symmetry in Chiral Recognition and Enantioselective Catalysis. Symmetry (Basel) 2014;6:210–21. https://doi.org/10.3390/sym6020210.
[47] Carrié D, Roisnel T, Simonneaux G. Asymmetric intermolecular cyclopropanation of alkenes and N–H insertion of aminoesters by diazoacetylferrocene catalyzed by ruthenium and iron porphyrins. Polyhedron 2021;205:115294. https://doi.org/10.1016/j.poly.2021.115294.
[48] Lo W, Che C, Cheng K, Mak TCW. Catalytic and asymmetric cyclopropanation of styrenes catalysed by ruthenium porphyrin and porphycene complexes. Chem Comm 1997;043:1205–6. https://doi.org/DOI https://doi.org/10.1039/A608080D.
[49] Frauenkron M, Berkessel A. A novel chiral ruthenium porphyrin as highly efficient and selective catalyst for asymmetric cyclopropanations. Tetrahedron Lett 1997;38:7175–6.

https://doi.org/10.1016/S0040-4039(97)01763-2.
[50] Galardon E, Roué S, Le Maux P, Simonneaux G. Asymmetric cyclopropanation of alkenes and diazocarbonyl insertion into S-H bonds catalyzed by a chiral porphyrin Ru(II) complex. Tetrahedron Lett 1998;39:2333–4. https://doi.org/10.1016/S0040-4039(98)00194-4.
[51] Gross Z, Galili N, Simkhovich L. Metalloporphyrin catalyzed asymmetric cyclopropanation of olefins. Tetrahedron Lett 1999;40:1571–4. https://doi.org/10.1016/S0040-4039(98)02647-1.
[52] Che C, Huang J, Lee F-W, Li Y, Lai T, Kwong H, et al. Asymmetric Inter- and Intramolecular Cyclopropanation of Alkenes Catalyzed by Chiral Ruthenium Porphyrins. Synthesis and Crystal Structure of a Chiral Metalloporphyrin Carbene Complex. J Am Chem Soc 2001;123:4119–29. https://doi.org/10.1021/ja001416f.
[53] Simonneaux G, Le Maux P. Optically active ruthenium porphyrins: chiral recognition and asymmetric catalysis. Coord Chem Rev 2002;228:43–60. https://doi.org/10.1016/S0010-8545(02)00009-7.
[54] Berkessel A, Kaiser P, Lex J. Electronically Tuned Chiral Ruthenium Porphyrins: Extremely Stable and Selective Catalysts for Asymmetric Epoxidation and Cyclopropanation. Chem - A Eur J 2003;9:4746–56. https://doi.org/10.1002/chem.200305045.
[55] Ferrand Y, Le Maux P, Simonneaux G. Highly Enantioselective Synthesis of Cyclopropylphosphonates Catalyzed by Chiral Ruthenium Porphyrins. Org Lett 2004;6:3211–4. https://doi.org/10.1021/ol048567y.
[56] Callot HJ, Piechocki C. Cyclopropanation using rhodium (III) porphyrins : Large vs selectivity. Tetrahedron Lett 1980;21:3489–92. https://doi.org/10.1016/S0040-4039(00)78722-3.
[57] O'Malley S, Kodadek T. Asymmetric Cyclopropanation of alkenes catalyzed by a "chiral wall" prophyrin. Tetrahedron Lett 1991;32:2445–8. https://doi.org/10.1016/S0040-4039(00)74349-8.
[58] Brown KC, Kodadek T. A transition-state model for the rhodium porphyrin-catalyzed cyclopropanation of alkenes by diazo esters. J Am Chem Soc 1992;114:8336–8. https://doi.org/10.1021/ja00047a081.
[59] O'Malley S, Kodadek T. Asymmetric cyclopropanation of alkenes catalyzed by a rhodium chiral fortress porphyrin. Organometallics 1992;11:2299–302. https://doi.org/10.1021/om00042a052.
[60] Teng P, Lai T, Kwong H, Che C. Asymmetric inter- and intramolecular cyclopropanations of alkenes catalyzed by rhodium D4-porphyrin: a comparison of rhodium- and ruthenium-centred catalysts. Tetrahedron: Asymmetry 2003;14:837–44. https://doi.org/10.1016/S0957-4166(03)00047-8.
[61] Anding BJ, Ellern A, Woo LK. Olefin Cyclopropanation Catalyzed by Iridium(III) Porphyrin Complexes. Organometallics 2012;31:3628–35. https://doi.org/10.1021/om300135f.
[62] Huang L, Chen Y, Gao G-Y, Zhang XP. Diastereoselective and Enantioselective Cyclopropanation of Alkenes Catalyzed by Cobalt Porphyrins. J Org Chem 2003;68:8179–84. https://doi.org/10.1021/jo035088o.
[63] Chen Y, Fields KB, Zhang XP. Bromoporphyrins as Versatile Synthons for Modular Construction of Chiral Porphyrins: Cobalt-Catalyzed Highly Enantioselective and Diastereoselective Cyclopropanation. J Am Chem Soc 2004;126:14718–9.

https://doi.org/10.1021/ja044889l.
[64] Chen Y, Zhang X. Trans Effect on Cobalt Porphyrin Catalyzed Asymmetric Cyclopropanation. Synthesis (Stuttg) 2006;2006:1697–700. https://doi.org/10.1055/s-2006-926450.
[65] Chen Y, Zhang XP. Asymmetric Cyclopropanation of Styrenes Catalyzed by Metal Complexes of D 2 -Symmetrical Chiral Porphyrin: Superiority of Cobalt over Iron. J Org Chem 2007;72:5931–4. https://doi.org/10.1021/jo070997p.
[66] Fantauzzi S, Gallo E, Rose E, Raoul N, Caselli A, Issa S, et al. Asymmetric Cyclopropanation of Olefins Catalyzed by Chiral Cobalt(II)-Binaphthyl Porphyrins. Organometallics 2008;27:6143–51. https://doi.org/10.1021/om800556v.
[67] Berkessel A, Ertürk E, Neudörfl JM. Asymmetric Cyclopropanation of Olefins Catalyzed by a Chiral Cobalt(II) Porphyrin. Org Commun 2017;10:79–89. https://doi.org/10.25135/acg.oc.11.17.04.019.
[68] Chen Y, Gao G-Y, Zhang XP. Palladium-mediated synthesis of novel meso-chiral porphyrins: cobalt-catalyzed cyclopropanation. Tetrahedron Lett 2005;46:4965–9. https://doi.org/10.1016/j.tetlet.2005.05.089.
[69] Chen Y, Ruppel J V., Zhang XP. Cobalt-Catalyzed Asymmetric Cyclopropanation of Electron-Deficient Olefins. J Am Chem Soc 2007;129:12074–5. https://doi.org/10.1021/ja074613o.
[70] Collman JP, Gagne RR, Halbert TR, Marchon J claude, Reed CA. Reversible oxygen adduct formation in ferrous complexes derived from a picket fence porphyrin. Model for oxymyoglobin. J Am Chem Soc 1973;95:7868–70. https://doi.org/10.1021/ja00804a054.
[71] Collman JP, Gagne RR, Reed C, Halbert TR, Lang G, Robinson WT. Picket fence porphyrins. Synthetic models for oxygen binding hemoproteins. J Am Chem Soc 1975;97:1427–39. https://doi.org/10.1021/ja00839a026.
[72] Tu W, Lei J, Zhang S, Ju H. Characterization, direct electrochemistry, and amperometric biosensing of graphene by noncovalent functionalization with picket-fence porphyrin. Chem - A Eur J 2010;16:10771–7. https://doi.org/10.1002/chem.201000620.
[73] Galardon E, Lukas M, Le Maux P, Simonneaux G. Synthesis and characterisation of a new chiral ruthenium picket-fence porphyrin and its use in chiral recognition of racemic isocyanides. Tetrahedron Lett 1999;40:2753–6. https://doi.org/10.1016/S0040-4039(99)00289-0.
[74] Jiang J, Yoon S. An aluminum(III) picket fence phthalocyanine-based heterogeneous catalyst for ring-expansion carbonylation of epoxides. J Mater Chem A 2019;7:6120–5. https://doi.org/10.1039/c8ta11877a.
[75] Sorokin AB. Phthalocyanine Metal Complexes in Catalysis. Chem Rev 2013;113:8152–91. https://doi.org/10.1021/cr4000072.
[76] Kobayashi N. Optically active phthalocyanines. Coord Chem Rev 2001;219–221:99–123. https://doi.org/10.1016/S0010-8545(01)00323-X.
[77] Engelkamp H, Middelbeek S, J. M. R, Nolte. Self-Assembly of Disk-Shaped Molecules to Coiled-Coil Aggregates with Tunable Helicity. Science (80-) 1999;284:785–8. https://doi.org/10.1126/science.284.5415.785.
[78] Okada Y, Hoshi T, Kobayashi N. Recent Progress in Optically-Active Phthalocyanines and Their Related Azamacrocycles. Front Chem 2020;8:1–14. https://doi.org/10.3389/fchem.2020.595998.
[79] Nemykin VN, Koposov AY, Subbotin RI, Sharma S. Preparation and characterization of first optically active rigid phthalocyanine dimers. Tetrahedron Lett 2007;48:5425–8.

https://doi.org/10.1016/j.tetlet.2007.06.016.
[80] Revuelta-Maza M, Torres T, Torre GD La. Synthesis and Aggregation Studies of Functional Binaphthyl-Bridged Chiral Phthalocyanines. Org Lett 2019;21:8183–6. https://doi.org/10.1021/acs.orglett.9b02718.
[81] Bächle F, Maichle- Mössmer C, Ziegler T. Helical Self- Assembly of Optically Active Glycoconjugated Phthalocyanine J - Aggregates. Chempluschem 2019;84:1081–93. https://doi.org/10.1002/cplu.201900381.
[82] Mu X, Wang D, Lu S, Zhou L, Wei S. Improved Photodynamic Activity of Phthalocyanine by Adjusting the Chirality of Modified Amino Acids. Mol Pharm 2022;19:115–23. https://doi.org/10.1021/acs.molpharmaceut.1c00672.
[83] Gök Y, Gök HZ, Karayiğit İÜ. Synthesis, characterization and aggregation properties of non-peripherally (1R,2R)-1,2-di(naphthalen-1-yl)ethane-1,2-diol substituted optically active zinc phthalocyanine and its catalytic application in enantioselective ethylation of aldehydes. J Organomet Chem 2018;873:43–9. https://doi.org/10.1016/j.jorganchem.2018.07.033.
[84] Gök Y, Gök HZ, Yılmaz MK, Farsak M, Karayiğit İÜ. Novel peripherally and non-peripherally hydrobenzoin substituted optically active phthalocyanines: Synthesis, characterization, aggregation, electrochemical properties and catalytic applications. Polyhedron 2018;153:128–38. https://doi.org/10.1016/j.poly.2018.06.053.
[85] Reetz MT, Jiao N. Copper-phthalocyanine conjugates of serum albumins as enantioselective catalysts in Diels-Alder reactions. Angew Chemie - Int Ed 2006;45:2416–9. https://doi.org/10.1002/anie.200504561.
[86] De Oliveira KT, De Assis FF, Ribeiro AO, Neri CR, Fernandes AU, Baptista MS, et al. Synthesis of phthalocyanines-ALA conjugates: Water-soluble compounds with low aggregation. J Org Chem 2009;74:7962–5. https://doi.org/10.1021/jo901633a.
[87] Lv W, Wu X, Bian Y, Jiang J, Zhang X. Helical fibrous nanostructures self-assembled from metal-free phthalocyanine with peripheral chiral menthol units. ChemPhysChem 2009;10:2725–32. https://doi.org/10.1002/cphc.200900547.
[88] Lv W, Zhu P, Bian Y, Ma C, Zhang X, Jiang J. Optically active homoleptic bis(phthalocyaninato) rare earth double-decker complexes bearing peripheral chiral menthol moieties: Effect of π-π interaction on the chiral information transfer at the molecular level. Inorg Chem 2010;49:6628–35. https://doi.org/10.1021/ic100552j.
[89] Romero MP, Gobo NRS, De Oliveira KT, Iamamoto Y, Serra OA, Louro SRW. Photophysical properties and photodynamic activity of a novel menthol-zinc phthalocyanine conjugate incorporated in micelles. J Photochem Photobiol A Chem 2013;253:22–9. https://doi.org/10.1016/j.jphotochem.2012.12.009.
[90] Lv W, Duan J, Ai S. "Pinwheel-like" phthalocyanines with four non-peripheral chiral menthol units: Synthesis, spectroscopy, and electrochemistry. Chinese Chem Lett 2019;30:389–91. https://doi.org/10.1016/j.cclet.2018.06.002.
[91] Sobotta L, Lijewski S, Dlugaszewska J, Nowicka J, Mielcarek J, Goslinski T. Photodynamic inactivation of Enterococcus faecalis by conjugates of zinc(II) phthalocyanines with thymol and carvacrol loaded into lipid vesicles. Inorganica Chim Acta 2019;489:180–90. https://doi.org/10.1016/j.ica.2019.02.031.
[92] Szymczak J, Sobotta L, Dlugaszewska J, Kryjewski M, Mielcarek J. Menthol modified zinc(II) phthalocyanine regioisomers and their photoinduced antimicrobial activity against Staphylococcus aureus. Dye Pigment 2021;193:109410. https://doi.org/10.1016/j.dyepig.2021.109410.

[93] Szymczak J, Rebis T, Kotkowiak M, Wicher B, Sobotta L, Tykarska E, et al. Regioisomers of magnesium(II) phthalocyanine bearing menthol substituents - Synthesis, spectral, electrochemical and computational studies. Dye Pigment 2021;191:109357. https://doi.org/10.1016/j.dyepig.2021.109357.
[94] Liu H-H, Wang Y, Shu Y-J, Zhou X-G, Wu J, Yan S-Y. Cyclopropanation of alkenes catalyzed by metallophthalocyanines. J Mol Catal A Chem 2006;246:49–52. https://doi.org/10.1016/j.molcata.2005.10.014.
[95] Kroitor AP, Cailler LP, Martynov AG, Gorbunova YG, Tsivadze AY, Sorokin AB. Unexpected formation of a μ-carbido diruthenium(IV) complex during the metalation of phthalocyanine with Ru3(CO)12 and its catalytic activity in carbene transfer reactions. Dalt Trans 2017;46:15651–5. https://doi.org/10.1039/c7dt03703a.
[96] Cailler LP, Kroitor AP, Martynov AG, Gorbunova YG, Sorokin AB. Selective carbene transfer to amines and olefins catalyzed by ruthenium phthalocyanine complexes with donor substituents. Dalt Trans 2021;50:2023–31. https://doi.org/10.1039/d0dt04090h.
[97] Kroitor AP, Dmitrienko AA, Martynov AG, Gorbunova YG, Sorokin AB. Substitution pattern in ruthenium octa-n-butoxyphthalocyanine complexes influence their reactivity in N–H carbene insertions. Org Biomol Chem 2023;21:69–74. https://doi.org/10.1039/D2OB01861F.
[98] de Jonge J, Bibo BH. The preparation of ortho and para hydroxybenzyl alkyl ethers. Recl Des Trav Chim Des Pays-Bas 1955;74:1448–52. https://doi.org/10.1002/recl.19550741202.
[99] Iranpoor N, Panahi F. Nickel-catalyzed one-pot deoxygenation and reductive homocoupling of phenols via C-O activation using TCT reagent. Org Lett 2015;17:214–7. https://doi.org/10.1021/ol503560e.
[100] Ghazal B, Machacek M, Shalaby MA, Novakova V, Zimcik P, Makhseed S. Phthalocyanines and Tetrapyrazinoporphyrazines with Two Cationic Donuts: High Photodynamic Activity as a Result of Rigid Spatial Arrangement of Peripheral Substituents. J Med Chem 2017;60:6060–76. https://doi.org/10.1021/acs.jmedchem.7b00272.
[101] Kroitor AP, Martynov AG, Gorbunova YG, Tsivadze AY, Sorokin AB. Exploring the Optimal Synthetic Pathways towards μ- Carbido Diruthenium(IV) Bisphthalocyaninates. Eur J Inorg Chem 2019;2019:1923–31. https://doi.org/10.1002/ejic.201900029.
[102] Sommerauer M, Rager C, Hanack M. Separation of 2(3),9(10),16(17),23(24)-Tetrasubstituted Phthalocyanines with Newly Developed HPLC Phases. J Am Chem Soc 1996;118:10085–93. https://doi.org/10.1021/ja961009x.
[103] Durmuş M, Yeşilot S, Ahsen V. Separation and mesogenic properties of tetraalkoxy-substituted phthalocyanine isomers. New J Chem 2006;30:675–8. https://doi.org/10.1039/b600196c.
[104] Ngubeni GN, Britton J, Mack J, New E, Hancox I, Walker M, et al. Spectroscopic and nonlinear optical properties of the four positional isomers of 4α-(4-tert-butylphenoxy)phthalocyanine. J Mater Chem C 2015;3:10705–14. https://doi.org/10.1039/C5TC01601K.
[105] Chen Y, Fang W, Wang K, Liu W, Jiang J. Nonperipheral Tetrakis(dibutylamino)phthalocyanines. New Types of 1,8,15,22-Tetrakis(substituted)phthalocyanine Isomers. Inorg Chem 2016;55:9289–96. https://doi.org/10.1021/acs.inorgchem.6b01371.
[106] Yanagisawa M, Korodi F, Bergquist J, Holmberg A, Hagfeldt A, Åkermark B, et al.

Synthesis of phthalocyanines with two carboxylic acid groups and their utilization in solar cells based on nanostructured TiO2. J Porphyr Phthalocyanines 2004;8:1228–35. https://doi.org/10.1142/S1088424604000581.
[107] Schoch TD, Mondal M, Weaver JD. Catalyst-Free Hydrodefluorination of Perfluoroarenes with NaBH4. Org Lett 2021;23:1588–93. https://doi.org/10.1021/acs.orglett.0c04305.
[108] Yamamoto S, Kuribayashi K, Murakami TN, Kwon E, Stillman MJ, Kobayashi N, et al. Regioregular Phthalocyanines Substituted with Bulky Donors at Non-Peripheral Positions. Chem - A Eur J 2017;23:15446–54. https://doi.org/10.1002/chem.201703105.
[109] Chandgude AL, Fasan R. Highly Diastereo- and Enantioselective Synthesis of Nitrile-Substituted Cyclopropanes by Myoglobin-Mediated Carbene Transfer Catalysis. Angew Chemie - Int Ed 2018;57:15852–6. https://doi.org/10.1002/anie.201810059.
[110] Zhang J, Huang X, Zhang RK, Arnold FH. Enantiodivergent α-Amino C–H Fluoroalkylation Catalyzed by Engineered Cytochrome P450s. J Am Chem Soc 2019;141:9798–802. https://doi.org/10.1021/jacs.9b04344.
[111] Fulmer GR, Miller AJM, Sherden NH, Gottlieb HE, Nudelman A, Stoltz BM, et al. NMR chemical shifts of trace impurities: Common laboratory solvents, organics, and gases in deuterated solvents relevant to the organometallic chemist. Organometallics 2010;29:2176–9. https://doi.org/10.1021/om100106e.
[112] Bruker AXS Inc., Madison, Wisconsin U. SAINT-Plus, Version 7.68 n.d.
[113] Bruker AXS Inc.: Madison, Wisconsin U. SADABS, version 2016/2 n.d.
[114] Dolomanov O V, Bourhis LJ, Gildea RJ, Howard JAK, Puschmann H. OLEX2 : a complete structure solution , refinement and analysis program. JApplCryst 2009;42:339–41. https://doi.org/10.1107/S0021889808042726.
[115] Sheldrick GM. SHELXT – Integrated space-group and crystal-structure determination. Acta Crystallogr Sect A Found Adv 2015;71:3–8. https://doi.org/10.1107/S2053273314026370.
[116] Sheldrick GM. Crystal structure refinement with SHELXL. Acta Crystallogr Sect C Struct Chem 2015;71:3–8. https://doi.org/10.1107/S2053229614024218.
[117] Mykhailiuk PK, Koenigs RM. Diazoacetonitrile (N2CHCN): A Long Forgotten but Valuable Reagent for Organic Synthesis. Chem - A Eur J 2020;26:89–101. https://doi.org/10.1002/chem.201903335.
.

Table of Contents artwork